55th JANNAF Propulsion Meeting, 12-16 May, 2008, Boston, MA (Draft: 5/2/08)

GASEOUS SURROGATE HYDROCARBONS FOR A HIFIRE SCRAMJET THAT MIMIC OPPOSED JET EXTINCTION LIMITS FOR CRACKED JP FUELS

Gerald L. Pellett*, Sarah N. Vaden[2], and Lloyd G. Wilson[3]

NASA Langley Research Center, Hampton, VA 23681

ABSTRACT

This paper describes, first, the top-down methodology used to define simple gaseous surrogate hydrocarbon (HC) fuel mixtures for a hypersonic scramjet combustion subtask of the HiFIRE program. It then presents new and updated Opposed Jet Burner (OJB) extinction-limit Flame Strength (FS) data obtained from laminar non-premixed HC vs. air counterflow diffusion flames at 1-atm, which follow from earlier investigations. FS represents a strain-induced extinction limit based on cross-section-average air jet velocity, U_{air}, that sustains combustion of a counter jet of gaseous fuel just before extinction. FS uniquely characterizes a kinetically limited fuel combustion rate. More generally, Applied Stress Rates (ASRs) at extinction (U_{air} normalized by nozzle or tube diameter, $D_{n\ or\ t}$) can directly be compared with extinction limits determined numerically using either a 1-D or (preferably) a 2-D Navier Stokes simulation with detailed transport and finite rate chemistry. The FS results help to characterize and define three candidate surrogate HC fuel mixtures that exhibit a common FS 70% greater than for vaporized JP-7 fuel. These include a binary fuel mixture of 64% ethylene + 36% methane, which is our primary recommendation. It is intended to mimic the "critical flameholding limit" of a thermally- or catalytically-cracked JP-7 "like" fuel in HiFIRE scramjet combustion tests.

Our supporting experimental results include: (1) An idealized kinetically-limited ASR reactivity scale, which represents "maximum strength" non-premixed flames for several gaseous and vaporized liquid HCs; (2) FS characterizations of Colket and Spadaccini's suggested ternary surrogate, of 60% ethylene + 30% methane + 10% *n*-heptane, which matches the ignition delay of a "typical" cracked JP fuel; (3) Data showing how our recommended binary surrogate, of 64% ethylene + 36% methane, has an identical FS; (4) Data that characterize an alternate surrogate of 44% ethylene + 56% ethane with identical FS and nearly equal molecular weights; this could be useful when systematically varying the fuel composition. However, the mixture liquefies at much lower pressure, which limits on-board storage of *gaseous* fuel; (5) Dynamic Flame Weakening results that show how oscillations in OJB input flow (and composition) can weaken (extinguish) surrogate flames up to 200 Hz, but the weakening is 2.5x smaller compared to pure methane; and finally, (6) FS limits at 1-atm that compare with three published 1-D numerical OJB extinction results using four chemical kinetic models. The methane kinetics generally agree closely at 1-atm, whereas, the various ethylene models predict extinction limits that average ~ 45% high, which represents a significant problem for numerical simulation of surrogate-based flameholding in a scramjet cavity. Finally, we continue advocating the FS approach as more direct and fundamental for assessing idealized scramjet flameholding potentials than measurements of "unstrained" premixed laminar burning velocity or blowout in a Perfectly Stirred Reactor.

---

* Senior Research Scientist, Hypersonic Air Breathing Propulsion Branch, Research and Technology Directorate. MS 168, NASA Langley Research Center, Hampton, VA 23681. Senior Member, AIAA g.l.pellett@larc.nasa.gov

[2] NASA-Langley Virginia Governor's School Participant, summer 2006; and LARSS student, summer 2007. Student at: Staunton River High School, Moneta, VA; and The Roanoke Valley Governor's School for Science and Technology, Roanoke, VA. Accepted at Georgia Tech, to begin July 2008.

[3] Technician, Lockheed Martin Space Operations, Hampton, VA

INTRODUCTION

For over 40 years, vaporized liquid hydrogen has been used almost exclusively in attempts to realize the potential of (airbreathing) Supersonic Combustion Ramjet (SCRAMJET) propulsion. Although liquid H_2 is difficult and expensive to use, it has remained the "fuel of choice," largely because of gaseous hydrogen's exceptional reactivity at near-atmospheric pressures, and in exceptionally lean mixtures. In addition, H_2 delivers a very high specific impulse, and has a uniquely high capacity for active cooling. On the other hand, vaporized liquid hydrocarbon (HC) fuels have so far been of limited use in hoped-for supersonic airbreathing applications, because they *are far less reactive*, even though they are obviously much easier to store and handle. Also, endothermic catalytic cracking of HC fuels has been investigated to improve both reactivity and cooling capacity [1-6]. However, difficult and competing performance challenges remain to achieve ignition and robust flameholding-combustion with various single component liquid HCs, jet fuels, and their surrogates injected just upstream of relatively small subsonic cavity flameholders, and also directly within them [4-25] – so as to (1) promote rapid initial reaction, with sufficient production and transport of radicals and (usually limited) enthalpy to the overriding supersonic shear layer, (2) avoid excessive internal drag and loss of net thrust, or much worse, loss of flameholding, and (3) achieve the needed "endothermic" heat soak and enhanced fuel reactivity in active cooling channels *without* the formation and deposition of significant carbon residues [3-6]. Thus thermally- or (more likely) catalytically-cracked fuel vapor and entrained air must partially mix, diffuse and react long enough in a subsonic cavity recirculation zone to achieve robust "incipient flameholding" (after auto- or spark-induced-ignition), to supply adequate radicals and enthalpy to the mainstream supersonic flow with minimal loss of kinetic energy.

Opposed Jet Burner (OJB) tools have been used extensively by the authors to measure the quasi-steady extinction limits of numerous laminar non-premixed, pure and N_2-diluted fuel vs air Counterflow Diffusion Flames (CFDFs) at one atmosphere [26-38]. Early efforts focused on: The velocity [36] and thermal structure [28,35], and strain-induced extinction of 14 to 100% hydrogen–air CFDFs, as summarized in Ref. 26; the efficacy of silane/hydrogen and silane/hydrocarbon mixtures for promoting ignition and piloting (without extinction) of very high speed combustion [27,33], including that in the Hyper-X vehicle; and the effects of contaminants in vitiated air from test facilities on H_2–air extinction limits [29-32,34]. The latter test effects were reviewed and used to assess possible differences in "incipient flameholding," compared to clean air in flight, in the subsonic re-circulating cavity flows of an otherwise supersonic combustor [39,40]. The CFDF studies showed that Flame Strength, FS, defined locally as the laminar maximum cross-section-average air input velocity, U_{air}, that sustains combustion of a particular counterflowing jet of gaseous fuel just before extinction, represents a unique and important fuel and air characterization parameter for chemical-kinetic-controlled extinction; and the FS limits effectively scale with hypothetical "idealized" scramjet flameholding limits [26,39,40]. Thus, the measured global Applied Stress Rates at extinction for either convergent-nozzle-OJBs (ASR_n) or straight-tube-OJBs (ASR_t), defined as U_{air} normalized by either nozzle or tube diameter, $D_{n\ or\ t}$, can be compared quantitatively with numerically simulated laminar extinction limits [26,35,36,41]. Such limits may be evaluated with reasonable accuracy using either a 1-D Navier Stokes stream-function approximation [see 26,37] with detailed transport and finite rate chemistry, or with greater accuracy for finite nozzles and tubes with prescribed inflow profiles, a fully detailed 2-D Navier Stokes numerical simulation [41].

New & Additional OJB Characterizations with HCs that Underlie Present Work

In our most recent paper [45], which followed [44] and earlier work [42,43], we conducted a logical progression of experimental and analytic studies that helped to define the combustion and extinction of gaseous HC–air CFDFs. Because some of these referenced results provide important bases for interpreting the current work, some key features are summarized in **Appendix A**, entitled "Supporting Strain Rate Characterizations."

Whereas [44] included FS results for six single-component hydrocarbon (HC) fuels (always pure, and also sometimes nitrogen-diluted), and also three HC-diluted H_2 fuels that showed very nonlinear decays in FS as HC was added, [45] was the first to characterize (a) *binary* mixtures (four) of pure simple HCs to identify linear and nonlinear interactions with ethylene, and other HC fuel candidates, and also (b) *ternary* mixtures (two) of simple HCs that included a vaporized liquid (*n*-heptane) at elevated temperature.

Thus, with increasing interest in HCs, both pure and mixed [3-25,42-49,55-57], and especially ethylene -- due to its high FS reactivity and its tendency to behave somewhat nonlinearly in mixtures (likely driven by the exceptional role of H-atoms) [45], and its continuing potential as a scramjet fuel component [13,16-19,59-62] -- it seemed important to extend the exploration of HC FSs. The study now includes additional mixtures of both gaseous and vaporized pure HCs, and *for the first time*, investigation of the Dynamic Flame Weakening (DFW) of a surrogate mixture and its pure components (i.e., our recommended 64% ethylene + 36% methane surrogate), at various frequencies from 10 to 1000 Hz.

Content of the Present Paper

This paper focuses initially on describing the methodology used to define simple gaseous surrogate fuel mixtures for an important subtask of the HiFIRE program. The technical problem is to help define a surrogate hydrocarbon (HC) fuel mixture, for a relatively sophisticated flight test configuration, that will effectively mimic the supersonic combustion behavior of an endothermically cracked JP-7 “like” kerosene fuel.

Thus, using a top-down approach, the paper first attempts to define the specific tests and planned uses of a HC surrogate fuel. Once these are delineated, comprehensive target bases for surrogate fuels are identified that relate to fuel properties, engine design characteristics, and basic and applied laboratory studies. After narrowing the primary focus to flameholding as a key critical element, some functional comparisons and distinctions are made between Scramjet flameholding, with a hypothetical cracked JP-7 “like” fuel, and Opposed Jet Burner (OJB) experimental data aimed at developing suitable gaseous surrogate mixtures.

Following our top-down definitional approach, the paper reviews some key findings in the recent literature pertaining to scramjet fuels and combustion, summarizes the authors’ recent comprehensive Flame Strength (FS) results on six mixed HC systems [45], and then presents three new data sets on two mixed HC systems. The authors’ recent FS results include four binary gaseous HC systems, including methane + ethylene, ethane + ethylene, methane + ethane, and methane + propylene; and two ternary vaporized HC systems that include both 10.8 and 21.3 mole % vaporized *n*-heptane (a “gold standard” among liquid fuels) *with* respective full ranges of methane + ethylene variation. The three new data sets include both FS *and* Dynamic Flame Weakening (DFW) results on the proposed 64% ethylene / 36% methane gaseous surrogate, and FSs of binary vaporized mixtures of *n*-heptane with *n*-dodecane, both “gold standard” liquid fuels.

More specifically, when we first set out to determine a simple gaseous surrogate [45], we found that *n*-heptane was the minor component of a tertiary surrogate fuel that had been proposed to mimic the ignition behavior of an endothermically cracked JP “like” kerosene fuel [6]. The composition of this “baseline simulant” (10 mole % *n*-heptane, 30% methane, 60% ethylene) was deduced and recommended by Colket and Spadaccini, based partly on detailed experimental shock tube data in their “Scramjet Fuels Autoignition Study,” and also on their pyrolysis and combustion experience with various JP fuels [6]. Thus, consistent with our proposed adoption of FS to gauge idealized scramjet HC flameholding limits [44], we focused particularly on characterizing FSs of the *entire n*-heptane + methane + ethylene system; and also comparable FSs of the ternary ethane + methane + ethylene system, the binary methane + ethylene system (preferred for high pressure storage), and the binary ethane + ethylene system

(with nearly constant molecular weight), as surrogate candidates for mimicking the “essential” flameholding behavior of an endothermic catalytically-cracked JP-7 “like” fuel [45].

Four major purposes are served by the new and updated FS (ASR) results: (1) The data from these HC mixtures provide sensitive and accurate means of validating, globally, complete and reduced chemical kinetic mechanisms. These apply at the critical flame core temperatures that determine non-premixed flame extinction, and also at the moderately elevated fuel inflow temperatures that are typically required to maintain fuel vapor; (2) The experimental FS and ASR scaling of results, while being directly helpful in validating and refining kinetic mechanisms, also support semi-quantitative assessments of the robustness and loss of “incipient” flameholding in scramjet combustors, for both pure and mixed HC fuels over wide ranges of reactivity; (3) The two simple binary gaseous surrogate fuel mixtures effectively allow substitutional bypassing of relatively complex vaporization and catalytic cracking system designs in test systems when supersonic combustion (scramjet) operability is the major goal; and perhaps most importantly, (4) The possibility of using binary surrogate mixtures of *variable* composition offers important additional test flexibility and research value; i.e., it allows well-defined and easily attained means of systematically varying fuel reactivity to effectively map the limits of robust and weak flameholding performance *with fixed geometry designs*.

Methodology used to Define Simple Gaseous Surrogates

We now focus on describing the methodology used to define simple gaseous surrogate fuel mixtures for the present surrogate fuel subtask of the HiFIRE program. The problem is to define a gaseous surrogate hydrocarbon (HC) fuel mixture, for a hypersonic scramjet flight test configuration, that can effectively mimic the supersonic combustion behavior of an endothermically cracked JP-7 “like” kerosene fuel.

Figs. 1 and 2 give a flow chart view of the process of “defining specific tests and uses of generic HC surrogate fuels” that might power a scramjet to Mach 8. For our present simplified short duration HiFIRE mission (~ 10 s powered flight), the goal is to achieve satisfactory vehicle performance with supersonic combustion of a simple gaseous HC fuel -- that behaves like an endothermically cracked fuel, while minimizing extraneous complex fuel processing. This means, not using a liquid fuel for active cooling with endothermic cracking, and thus dispensing with the technologies and hardware required for fuel processing.

Thus in Figs. 1 and 2 we down-select to the rapid blowdown of gaseous (not supercritical) HC fuel from a carbon composite tank, at 4000 psi, that is only mildly heated (< 100 deg C). Passive preheat is then available to maintain a gaseous state through blowdown and injection at ~ 400 psi via a heated manifold. Autoignition will *not* be relied on, but spark induced ignition will. At this point, robust flameholding is judged to be most critical. However, “at the other end,” if the heat release of flameholding with localized combustion becomes excessive in conjunction with upstream boundary layer combustion, so-called “unstart,” i.e., in the engine inlet, can also become critical [8-10,13,16-19].

Figs. 3a and 3b delineate a comprehensive set of “target bases for surrogate fuels *after* the primary use is specified.” These target bases relate to Fuel Properties, Engine Design / Characteristics, and basic and applied Laboratory Studies. Many represent important features to be considered for measurement and testing in detailed analyses of any complex system. Although there are several different Laboratory Studies of premixed flames that shed light on important combustion characteristics of a fuel (Fig. 3b), this study has focused on non-premixed flames -- and in particular -- their extinction limits near atmospheric pressure, as the first critical feature to characterize and compare for possible HiFIRE application. Thus, the extinction limits of non-premixed flames are considered most representative for ranking the strain-rate-limited combustion rates in highly strained flameholding regions of a cavity flameholder.

Now that the primary “target base” in Fig. 3a has been narrowed to flameholding as a principal critical element under “engine design / characteristics,” the extinction of non-premixed

combustion in Fig. 3b is identified as a key feature of experimental "laboratory studies." Finally, Fig. 4 helps define some "functional comparisons" and distinctions between Scramjet flameholding with a hypothetical cracked JP-7 "like" fuel and the present OJB experimental approach, aimed at developing suitable gaseous surrogates. All six of the functional "characteristics of flameholding" are affirmative with respect to both "scramjet with cracked JP-7" and "opposed jet with gas surrogate."

We now proceed with the experimental part of the study to review and identify candidate gaseous surrogate HC mixtures that satisfy the logical development described above.

EXPERIMENTAL

Schematics, with detailed descriptions, are given for the nozzle-OJB system that was used (vertical orientation with a selectable Oscillatory-inflow delivery) in the Oscillatory Opposed Jet System (OOJB) in Fig. 5a; a recent horizontal tube-OJB system, Fig. 5b; and the liquid HC vaporizer-accumulator-OJB system, Fig. 5c. All three systems depict the use of convergent Pyrex nozzles, and long nickel or stainless steel tubes (50 to 100 diameters in length), of the same size and type. No guard flows were used (or seemed to be needed) at the typical flow rates employed for extinction of thin disk-shaped flames. Although horizontal configurations sometimes showed a slight flame asymmetry due to buoyancy (but negligible differences in results) [33], they favored formation of resultant ring-shaped flames, and thus allowed measurements of flame restoration, which approximate a slightly strained laminar burning velocity (discussed below). Each ceramic fiberboard combustion box had Pyrex windows, and a porous sintered metal plate over the top. Nitrogen (or argon) entering through diffuser-jets at the bottom of each box reduced extraneous combustion outside the central impingement region, and thus minimized adverse buoyancy and visibility effects. Fuel and air component flows were hand-controlled with micrometer valves, and measured by mass flow meters calibrated for air at 0 ^{o}C, 1-atm pressure. Vendor-published mass flow meter correction factors (either measured relative to air or evaluated as ratios of heat capacities) were used for calculating mole fractions of HC mixtures involving ethane, propane, butane and propylene. Similar published factors for methane and ethylene were found to have significant error, and were thus evaluated independently in a series of carefully controlled experiments [45].

To attain extinction (blowoff) of a stabilized gaseous fuel–air disk flame, the fuel flow rate was gradually increased (or, for N_2 diluted fuels, fixed at a target rate as N_2 diluent was increased); simultaneously, the airflow was gradually increased, so that the flame was always centered and free-floating (fully responsive to small differential changes in flow rates). Upon sudden blowoff, a ring-shaped (torus) flame sometimes stabilized. After mass flows of each component were recorded, gradual flow reductions led to slow closure of the ring flame, and eventually, to sudden disk restoration (see Ref. 26 for a summary of the author's earlier CFDF restore results, and Ref. 58 for a recent independent study). Extinction data were almost always obtained in duplicate, and were sometimes replicated 10 or more times, especially in the case of heated / vaporized liquid fuels. Here, premixed (with N_2, or one or two gaseous HCs) vaporized-HC flows from the pressurized accumulator system, Fig. 5c, were simply varied in tandem with flows of air to achieve extinction. Similar procedures were applied for mixed gaseous H_2/HC–air and HC_1/HC_2–air systems, in that H_2 or one HC diluent / reactant was fixed, while the other was gradually increased in tandem with air to achieve extinction.

Reported exit cross-section-average jet velocities, U_{air} and U_{fuel}, are calculated from the measured component mass flow rates, flow meter calibration factors for each gas, and carefully measured nozzle or tube exit diameters. Mass flow meter calibrations of airflow rates are referenced to 0 ^{o}C and 1-atm, but are then corrected to 300 K (ideal gas law) and 1-atm [44]. Corresponding Reynolds numbers for air (Re_{air}) based on diameter were generally less than 1500, but considerably lower values were avoided; especially because flames can become

excessively thick when vertical, and also non-axisymmetric when horizontal, due to buoyancy. Radiation effects were considered negligible at the relatively high strain rates used.

The matched tube-OJBs (7.56 mm diameter mostly, but ranging from 2.7 to 10.0 mm in previous studies) were mounted horizontally. The 7.2 mm Pyrex nozzles were mounted vertically, with both elements insulated to reduce heating of the inflowing gases.

The 7.5 mm tube- and 7.2 mm nozzle-OJBs were spaced 1.7 to 2 exit-diameters apart (note that the extinction limits are exceptionally independent of jet separation distance beyond one diameter, and sometimes up to 4 diameters [26]). For measurements with H_2, both the 2.7 and 2.91 mm OJB's were 7 mm apart to ensure free-floating finite-thickness flames, free of significant flame attachment / anchoring effects. Flow rates were generally high enough that buoyancy and OJB orientation effects on flame extinction appeared negligible [26,33,43-45] whenever data were recorded. Vaporized-HC fuel mixtures flowed through the electrically heated vaporizer and accumulator tanks and tubes with thermocouple monitoring (see Fig. 5c), before entering the OJB combustion chamber, so that these fuels were heated up to ~ 600 K to prevent condensation.

Several checks were also made on possible temperature–time degradation effects on HCs [44,45]. The checks included propane–air ASR extinction limits, using 300 K air and unheated propane (101.4 1/s at 300 K); rapidly heated propane (105.2 1/s for $\leq$ 0.1 hr at 600 K), and long-term-heated propane (104.4 1/s for ~ 2 hr at 600 K). These results showed a small increase in ASR due to heating (3.8% ave), and a negligible difference (~ 1.5%) that might be ascribed to possible decomposition effects (short- vs long-term "cooking") [44,45]. Similar checks on possible degradation were conducted on both ethylene and methane, with similar results (described later).

Errors in extinction limits stemmed from various sources. In earlier studies of the H_2–air system, *absolute* strain rates at extinction (not density weighted) were predicted (1-D) to vary linearly with input temperature, up to ~ 600 K [50,51], and *absolute* ASRs for heated H_2–air, using a 2.7 mm tube-OJB, were found to vary "nearly" linearly (e.g., with only a 14% excess increase in density-weighted ASR from 300 to 600 K [38]). Thus, direct measurements of mass flow rates effectively negated most effects of variable jet temperature on *absolute* jet velocity via the ideal gas law. This led to significant reduction of data scatter, especially when input heating was required. Atmospheric pressure variations caused small variations of U_{air} extinction limits that were generally ignored and averaged-out during earlier hydrogen studies [26], but more recent HC and H_2 data were corrected by applying a dimensionless pressure factor of $(1/P)^{+3}$ [44]. Calculated (density-weighted) jet exit velocities at standard conditions varied inversely as the square of measured D, and ASRs varied as D^{-3}. Finally, un-reconciled small differences between the data sets were due to earlier unmeasured variations in atmospheric pressure, differences in centering flames, daily jet realignment, sporadic but generally small mass flow meter drift, periodic mass flow meter calibrations, small transient cooling / heating flow response effects in flow meters, and differences in the spatial distribution and flow rates of argon or nitrogen purge flows in the combustion box.

Finally, because jet-edge velocity-mismatch and resultant bath gas entrainment / diffusion effects were *incipient and evident* at high H_2 concentrations with the 2.7 mm nozzle-OJB [26], and also the flame thickness at extinction was as large as ~ 1/3 D, the greatest uncertainty and non-ideality in our previous H_2–"clean air" extinction studies [26] is now believed to be associated with the 2.7 mm Pyrex nozzle-OJB. On the other hand, the 2.7 and 2.9 mm tube-OJBs performed much more ideally due to lack of significant "velocity-mismatch" at each jet's edge.

In summary, relatively ideal and well characterized 7.56 mm tube-OJB and 7.2 mm nozzle-OJB systems were the primary tools used in this study for assessing strain-induced extinction limits of gaseous and vaporized-liquid HC–air CFDFs.

RESULTS AND DISCUSSION

OJB-Extinction "Flameholding Scale" for Pure and Mixed Gaseous HCs

Fig. 6 shows the Applied Stress Rate (ASR) data at extinction for binary **methane + ethylene** and **ethane + ethylene** fuel mixtures vs air, using a 7.56 mm Tube-OJB with 1-atm, 300 K inputs. Flame extinction occurred at each data point, and thus the data fits define upper ASR boundaries beyond which flame cannot exist. The nonlinearity in each system is reminiscent of much larger nonlinearities seen earlier in HC + H_2 systems [44], in that they may reflect a degree of scavenging of H-atoms from ethylene decomposition by HCs stemming from methane and ethane. The mild nonlinearity exhibited in the present methane + ethylene system, and the strong nonlinearity in the methane + H_2 system [44], was recently "confirmed" in numerical simulations [60,61] using contemporary chemical kinetics models (discussed later). Note that ethane, compared to methane, has a significantly higher FS, a lower vapor pressure at ambient temperature, and approximately the same molecular weight as ethylene (30 vs 28). All three properties can affect the design and operational performance of a binary gaseous surrogate-FS composition.

More specific chemical explanations of the nonlinear extinction limits in Fig. 6 may be evident from further application of refined global chemical kinetic formulations (recently there are more than three), however, detailed sensitivity and reaction path analyses are probably needed in addition to numerical simulations of the OJB extinction limits. Similar considerations also apply in far more complex fuel systems, in which the detailed chemical kinetics are sometimes extremely complicated [13-19,22,24,25], and where both kinetics and diffusion may play critical and competing roles [17,18].

Fig. 7 shows the ASR data for the **methane + ethane** system, which, instead, exhibits *highly linear* behavior with the mole fraction of ethane. This (somewhat expected) result suggests combustion of these simple aliphatic HCs proceeds as if the two HCs behave independently, and in proportion to their molecular abundance.

Note the above three systems in Figs. 6 and 7 constitute a simple ternary system that can be completely characterized, analytically, without the need for additional ternary-mapping data, *if* a relatively simple and reasonable assumption is made. That is, the linearity involving methane + ethane in Fig. 7 (for zero ethylene) is also assumed to hold for all sets of mixtures in which ethylene mole fraction is constant. Thus an analytic surface was constructed [45] consisting of an infinite number of straight lines that connect the respective parabolic fits of methane + ethylene, and the ethane + ethylene systems, on lines of constant ethylene mole fraction.

Fig. 8 shows the ASR data for the **methane + propylene** system, which also exhibits highly linear behavior with mole fraction propylene. These data are somewhat surprising in two respects: First, the ASR for 300 K propylene–air at extinction (107 1/s) is about 2x lower compared to 300 K ethylene (212 1/s), *and* second, the mixed fuel system behaves linearly with mole fraction. Again, a kinetic explanation is sought.

Fig. 9, a cross-plot of ASRs for all the pure gaseous HCs at 300 K, adds a new gas obtained independently with *both* nozzle- and tube-OJBs (the 64%/36% ethylene/methane surrogate) to the previous cross-correlation [45]. Thus, Fig. 9 shows OJB-extinction-limits for *seven* pure gaseous HCs on the linear "Idealized Flameholding Scale." All the ASRs were obtained using the 7.2 mm convergent Pyrex nozzle-OJB and a 7.5 mm straight tube-OJB (except for two sets of methane–air data from a 5.1 mm Pyrex nozzle and a 5.0 mm tube). Also, all the results represent averages of significant multiple-entry determinations. Slight corrections in data points were made recently for C_3H_6, and a new point and average appears for CH_4, as a result of data rechecks, after a leak was discovered and fixed (due to a crack in the airside speaker). Thus, all the nozzle-OJB FS data in Fig. 9 were carefully reviewed and re-checked, along with in-series air

mass flow checks. Obviously, ethylene exhibits by far the highest Flame Strength (ASR) of any HC tested (acetylenes have not been run).

Translation of global strain rates to absolute axial input strain rates

We now translate easy-to-measure global OJB strain rates (ASRs) into *more generalized* absolute axial input strain rates, at the airside edge of a CFDF, which (typically) represent the outputs of detailed 1-D (and 2-D) numerical simulations, subject to various boundary conditions. A similar (but much more difficult, and less certain) approach may be taken for the translation of global OJB strain rates to radial strain rates *in the so-called flame core* (generally not located at the stagnation point). Flame-core radial strain rates constitute the "truest representation" of the strength of CFDFs, but they are by far the most difficult to measure using non-intrusive laser diagnostics, and model using more intensive 2-D simulations.

To begin the translation, we first examine *carefully* the relationship between the respective *hydrocarbon* extinction limits for plug-inflow (nozzle based) and parabolic-inflow (tube-based) ASRs in Fig. 9. This affects the scaling of respective global strain rates to axial strain rates *on an absolute basis* (also assessed independently using earlier Particle Image Velocimetry (PIV) and Laser Doppler Velocimetry (LDV) with the present OJBs [26,35,36]). First, we note the curve fit in Fig. 9 has a slope (2.53) that relates independent ASRs from nozzle-OJBs, ASR_n, to those from tube-OJBs, ASR_t, *but* it has a significant intercept. Alternately, Fig. 10 shows the same data plotted with a forced zero intercept. Although the latter fit is not quite as good statistically, ASR_n = 2.23 ASR_t effectively characterizes the absolute linearity of the relationship between plug-inflow and parabolic-inflow HC extinction results. Note that the factor 2.23 agrees with an average ASR ratio for *hydrocarbon*–air extinctions in Fig. A3 (shown later), but *it differs considerably* from that for N_2-diluted H_2 fuels. This is because the uniquely high rate of H_2 diffusion causes the high temperature core of a H_2 flame to locate significantly farther upstream on the airside of the stagnation point, where the local radial strain rate is lower than that at the stagnation point, due to reduced flow divergence -- discussed in Appendix A. Now, the 2.23 ASR ratio for HC–air CFDF extinctions is needed to complete the conversion.

Next, we examine three independent sources of relevant strain rate data: (1) Rolon's careful strain rate measurements of cold laminar "plug flows" of air vs air, using 25 mm diameter convergent nozzles (discussed in Appendix A; shown in Fig. A1); (2) our earlier PIV and LDV measurements of axial (and radial) strain rates, using 7.2 mm nozzle- and 7.5 mm tube-OJBs, that are consistent with plug inflow SRs being ~ 2.5 x larger than parabolic inflow SRs at the same average inflows [26,36]; and (3) Hwang's 2-D numerical simulations of opposed plug and parabolic inflows with equal mass flows [41] (see footnote below[1]). Based on Rolon's and Hwang's results, we adopt a common "independently verified" proportionality (1.15) between the maximum axial strain rate input on the airside, $-(1/2)\,(du/dx)_{max}$, and the global ASR_n for a nozzle-OJB. In using the average value of 1.15, we can write (using the present nomenclature)

$$-(1/2)\,(du/dx)_{max} = 1.15\ ASR_n = \mathbf{1.15}\ U_{air}/D_n \qquad (1)$$

[1] Hwang's 2-D numerical simulations of cold (300 K) plug and parabolic OJB impingement flows (with jet separation $H = D$) to determine respective axial and radial strain rates (velocity gradients) result in the following [41]: $-(1/2)\,(du/dx)_{max} = \mathbf{1.152}\ U_{air}/D_n$, and $(dv/dr)_{max} = \mathbf{1.158}\ U_{air}/D_n$ for **plug** inflows; and $-(1/2)\,(du/dx)_{max} = \mathbf{2.530} * 1.152\ U_{air}/D_t = \mathbf{2.91}\ U_{air}/D_t$; and $(dv/dr)_{max} = \mathbf{2.528} * 1.158\ U_{air}/D_t = \mathbf{2.93}\ U_{air}/D_t$ for **parabolic** inflows. Note that we previously deduced 3.0 (which is close to 2.91) from LDV and PIV surveys [26,35,36]. Thus -1/2 the maximum axial strain rate equals a common radial strain rate for both plug and parabolic inflows, and the respective axial and radial strain rates for plug inflows differ from the parabolic inflows by a ratio of **2.53**, which matches the slope (2.53) in Fig. 9 and is quite close to the zero-intercept slope (2.23) in Fig. 10.

and then substitute the experimentally demonstrated proportionality in Fig. 10 for gaseous HCs, $ASR_n = 2.23\ ASR_t$. By doing so, we define a globally based measure of maximum axial strain rate at the airside edge that can be used later to compare experimental with computational results,

$$- (du/dx)_{max} = \mathbf{2.30}\ U_{air}/D_n = 2.30 * 2.23\ U_{air}/D_t = \mathbf{5.13}\ U_{air}/D_t \qquad (2)$$

In comparison, note that Hwang's 2-D numerical simulations using equal cold mass flows [41] show the linear proportionality between opposed 5.0 mm nozzle (plug) inflows and tube (parabolic) inflows as $ASR_n = 2.53\ ASR_t$; and moreover the 2.53 applies not only for axial strain rates on the airside, but also for radial strain rates at the stagnation point. Perhaps coincidentally, the slope in Fig. 9 is 2.53. Furthermore, for Hwang's numerically simulated H_2–air extinction "hot flows," the ratio of axial input strain rates for (equal mass flow rate) opposed 3.0 mm nozzle and 3.0 mm tube flows is also very close to 2.5 [41].

In conclusion, we have derived empirical expressions that should quite accurately relate global ASRs, for laminar nozzle- and tube-OJB inflows, to maximum axial strain rate inputs at the airside edge of opposed cold and HC–air CFDFs. These should allow reasonably accurate comparisons of global experimental data with either numerically evaluated strain rates or measured maximum axial strain rates at extinction.

Extinction of Vaporized *n*-Heptane, *n*-Dodecane, JP-7 & JP-10 Fuels

Fig. 11 shows new ASR extinction results for vaporized mixtures of *n*-dodecane with *n*-heptane, in mole fractions of 1.0 and 0.5; and also 0 for pure *n*-heptane, obtained previously [45]. The *n*-dodecane has a FS nearly 17% higher than *n*-heptane, and the FSs appear highly linear on a molar composition scale, which is not surprising considering that both are similar aliphatic HCs.

The above ranking is at least qualitatively consistent with *projections* of published extinction data on these HCs when they are highly-N_2-diluted. For example, Fig. 12 shows (on the left side) a very limited comparison with non-premixed N_2-diluted HC vs air extinction limits for 4-11 mole % *n*-dodecane (solid-squares) [14], and 18 and 25 mole% *n*-heptane (solid-circles) [55]. These results were obtained at different times from a Seshadri matrix-type OJB with very closely spaced nozzles [54] – which, for comparison purposes, require a substantial strain rate correction, that is described below after the present authors' OJB data are discussed.

Fig. 12 also contains the authors' newly obtained *n*-dodecane data, plotted along with their previous results [42-45] on pure and N_2-diluted *n*-heptane and JP-7, and pure JP-10 fuels. The apparatus and general procedures used are shown and described in Fig. 5c. The respective ASRs for N_2-diluted *n*-heptane and JP-7 increase substantially with increasing HC mole fraction, up to ~ 75 mole %; thereafter, the ASRs attain respective asymptotic values, just like the gaseous HCs and hydrogen fuels do. These asymptotes suggest, as before, that *chemical kinetic-limited* ASRs are attained, because each is unaffected by significant decreases in local N_2 dilution and diffusion flux beyond 75 mole %. Although all four fuels are of higher molecular weight and lower diffusivity than the simple gaseous HCs and H_2, and the flames (with axial-momentum-balanced input flows of $\rho_{air} * U_{air}^2 = \rho_{fuel} * U_{fuel}^2$) should lie closer to the stagnation point, subsequent fuel pyrolysis and combustion kinetics of lower molecular weight fuel species in the airside flame should continue to be affected by N_2 dilution and diffusion from the fuel side.

As indicated above, the solid-circle data in Fig. 12, which agree reasonably well with the authors' *n*-heptane data, represent substantially corrected experimental extinction strain rate (SR) results from Seiser et. al [55], who used a 22 mm diameter matrix-OJB with a gap of H = 10 mm. The same applies for the solid-squares *n*-dodecane data in Fig. 12 from Hummer et. al [14]. Thus the plotted extinction results in [55] (and [14]) were corrected in two steps to be comparable with the present ASR scale for a tube-OJB, as discussed in Appendix A regarding Fig. A1. First, based on Rolon's measurements of -1/2 axial and radial SRs as a function of nozzle separation distance

[52], a correction factor of 1/0.42 was applied to the matrix-OJB "global SR" results of 500 1/s for 25 mole % *n*-heptane/N_2–air, and 400 1/s for 18 mole % *n*-heptane/N_2–air in Ref. [55]. The 1/0.42 factor estimates the *actual* radial (and -1/2 axial) SRs that "effectively" existed at H/D_{burner} = 0.45 -- as a correction of the "standard SR expression" in Refs. 54 and 55 for a matrix-type burner, $2U_{air}/H$, that assumes no radial gradients at the nozzle exits, a linear axial SR profile between the nozzles, and an axial momentum balance for cold inflows. Next, SRs from the first stage of correction, which allowed comparisons with uniform velocity (plug flow) ASRs from a convergent nozzle, were also divided by a factor of 2.5. This approximated both the experimentally- and numerically-derived factor (discussed above re: Figs. 9 and 10) that converted plug inflow ASRs for hydrocarbon–air systems to equivalent parabolic-inflow ASRs with the *same* radial strain rate in the flame core (see also [41]). As noted earlier, because the equivalent H/D_{burner} = 0.45 separation of 11.25 mm in Fig. A1 is a little smaller than Rolon's smallest separation (15 mm), and Rolon's flows were cold, the first part of the correction (1/0.42) is a slightly-extrapolated best approximation.

Comprehensive "Idealized Flameholding Scale" for HCs, H_2 and Mixtures

Fig. 13 shows the extension of the linear "Idealized Flameholding Scale" of Fig. 9 for HCs (w/intercept), by summarizing the new and previous [42-45] extinction ASRs for *all* the pure gases, the various vaporized-HC fuels that were sometimes N_2-diluted, and the earlier H_2–air and H_2/HC–air data. Three sets of the vaporized-HC data from Fig. 12, that apply for 100% JP-10–air, both pure and nitrogen-diluted JP-7, and *n*-heptane, were originally shown in [42,43], but the mole fractions for N_2-diluted mixtures were slightly revised in [44] and [45].

Thus, Fig. 13 shows a 50-fold range of normalized ASR's for various "pure" vaporized-liquid and gaseous hydrocarbons in ascending order of reactivity: JP-10, methane, JP-7, *n*-heptane, *n*-butane, propane, propylene, ethane, 64%/36% ethylene/methane surrogate mixture, and pure ethylene. Pure hydrogen produces a unique and exceptionally strong flame at the extreme upper end of the flameholding scale (see also Fig. A3). Both H_2 data points (averaged from previous 2.7 mm Pyrex nozzle- and 2.7 mm tube-OJB data, and also from a recent 2.91 mm tube-OJB) agree within about 1% of Hwang's recent 2-D numerically simulated ASR_t for H_2-air extinction, for a 3.0 mm tube-OJB configuration, with appropriate guard flows and disk-shaped boundary conditions [41]. For all the data points marked with a pound sign (#), measurements made with tube-OJBs were plotted on a least-squares fit of all the gaseous HC data *and* the data for pure H_2 as described above. Although the linear slope (with intercept) increased from 2.53 to 2.73 due to addition of pure H_2 data, the former slope (2.53) is considered to be more appropriate for HC CFDFs, due to the previously discussed effect of a downstream shift in the average HC flame location on the airside, relative to that for hydrogen.

Based on the above FS and ASR characterizations, including the 50 x range of linear reactivity between JP-10 and H_2 exhibited on the "Idealized" flameholding scale of Fig. 13, we reiterate our earlier conclusion [44,45] that the respective nozzle- and tube-inflow ASRs, and ratios of ASRs for various "pure" hydrocarbons and hydrogen, effectively represent global chemical kinetic limits. And, as such, the ASRs provide relative and absolute tests of the efficacy of reduced chemical kinetic models, when applied at the appropriate pressures and peak flame core temperatures of extinction.

Extinction Results for Hot (600 K) Methane + Ethylene + *n*-Heptane Mixtures

Pellett et al. systematically presented comprehensive extinction data for hot (600 K) ternary mixtures of methane + ethylene + *n*-heptane [45]. The authors analyzed the results to define the FS (and ASR_t = 160 1/s) of Colket and Spadaccini's proposed "baseline simulant" for endothermically-cracked JP-7 "like" kerosene [6], namely 10 mole % *n*-heptane + 60% ethylene + 30% methane. The extinction results for hot mixtures of methane + ethylene and ethane + ethylene were then presented to determine a binary surrogate mixture of 64% ethylene + 36% methane that exhibits the same ASR_t at extinction, as well as an alternate binary surrogate of 44% ethylene + 56% ethane having the same ASR_t. Although some of the key results of the

original investigation are presented below for the sake of completeness, additional details may be found in the paper [45].

High temperature extinction measurements for both methane and ethylene were obtained to determine "cooked fuel" ASRs at the same elevated temperatures used to vaporize liquid fuels. Thus, Fig. 15 shows a "higher fuel temperature" version of the Fig. 6 ASR_t data at extinction, for binary **methane + ethylene** fuel mixtures vs air, using a 7.56 mm Tube-OJB at 1 atm, with 300 K air inputs *and* fuel inputs at $\geq$ 600 K. This "hot" version was obtained after both pure methane and pure ethylene charges were heated in the same accumulator system to $\geq$ 600 K for $\geq$ 1 hr, at ~ 70 psia, to obtain high temperature ASR_t data at each extreme. Then, the Fig. 6 data were temperature-corrected by applying resultant linear (interpolated) factors to the ASR_t results at intermediate mole fractions, as described in Ref. [45]. Note the markers showing the FS of the 64% ethylene + 36% methane surrogate and the FS of vaporized JP-7.

Additional experiments were conducted to directly assess possible thermal *and* HC-decomposition effects on ASRs. Thus the respective data averages were determined for "cooked," "rapidly-heated," and "cold" fuels as follows.

The respective ASRs (1/s) obtained for **methane** were: **80.9** $\pm$ 0.6 for $\geq$ 1 hr at 630 K; **81.0** $\pm$ 0.6 for ~ 0.1 hr at 630 K; and **80.4** $\pm$ 0.4 at 300 K. (Bold notation is used to highlight the main results.) These ASRs show a negligible effect of both temperature and heating time in our system, which is characterized by a very low effective average surface to volume ratio, compared to flow in typical small tubes. In fact, the results closely resemble the earlier ones for **propane** [42,43] that were: **104.4** $\pm$ 1.1 for $\geq$ 1 hr at 600 K; **105.2** $\pm$ 0.4 for $\sim$ 0.1 hr at 600 K; and **101.4** at 300 K. Finally, the respective ASRs (1/s) for **ethylene** were: **228.4** $\pm$ 1.5 for $\geq$ 1 hr at 620 K; **226.1** $\pm$ 0.7 for $\sim$ 0.1 hr at 640 K; and **211.3** $\pm$ 5.9 at 300 K. These show negligible difference between cooked and rapidly heated ethylene, but together they average about 7.5 % higher than for cold ethylene. As indicated earlier, the "hot" ASRs for methane and ethylene were used to correct the cold ASR data in Fig. 6 to hot ASRs in Fig. 15.

Fig. 16 shows ASRs at extinction for ~ 600 K ternary mixtures of **10.8 $\pm$ 0.3 mole % *n*-heptane + methane + ethylene** vs 300 K air. Note the datum point that characterizes an ASR corresponding to Colket and Spadaccini's simulated endothermically-cracked JP-7 "like" kerosene [6]. Careful chemical kinetic modeling is needed for the ternary system, once the binary gaseous system has been successfully characterized.

Fig. 17 shows ASRs at extinction for similarly hot ternary mixtures of **21.3 $\pm$ 0.5 mole % *n*-heptane + methane + ethylene** vs 300 K air. The data trends, including intercepts, are an unremarkable extension of Figs. 15 and 16, but they enable a more comprehensive and accurate fit of the ternary system.

Fig. 18 shows ASRs at extinction for hot binary mixtures of ***n*-heptane + ethylene** vs 300 K air. The data fit provides a zero-methane baseline for the hot ternary system. Note the results from the three different test conditions (described above) for pure ethylene, that were used to assess possible thermal and ethylene-decomposition effects on ASR at elevated fuel temperatures (~ 630 K).

Fig. 19 shows ASRs at extinction for hot binary mixtures of ***n*-heptane + methane** vs 300 K air, which provides a zero-ethylene baseline for the hot ternary system. Although these data are less extensive at intermediate concentrations, and the actual data trend may slightly be non-linear, the ASR difference spanned is not great. Note the results from the three different test conditions for pure methane, which show negligible thermal and methane-decomposition effects on ASR at elevated fuel temperatures (~ 630 K).

Fits of Hot Methane + Ethylene + *n*-Heptane System; Definition of Surrogates

The above five sets of ASR_t extinction data in Figs. 15-19, that apply to the hot (600 K) ternary system of methane + ethylene + *n*-heptane, were analyzed to produce analytic polynomial fits of 3-D surfaces that applied over the entire range of fuel compositions. Thus, the ASR that best corresponded to the Colket and Spadaccini "reformed fuel" or "baseline simulant" composition (ASR_t = 160 1/s) was used to deduce the composition of a hot binary methane + ethylene surrogate that exhibited the same ASR. The resultant "best fit" was 64% ethylene + 36% methane. A simple inspection of Figs. 15 and 16 confirms this finding. Details of the analysis can be found in Ref. 45.

Planned Fuel Cracking Studies Related to the Present Surrogate

Presently, the authors are setting up an isothermal-decomposition sub-system to process (and crack) hot mixtures just before they enter the OJB, so that the question "what actually is the achievable Flame Strength of a cracked JP-7" can be addressed. Note, from the measured ASR_t = 93 1/s for "pure" JP-7, that the 160 1/s surrogate represents a 70% increase in ASR for a "cracked" JP-7; this compares with 227 1/s for pure ethylene (all fuels at 600 K). Whether or not it is possible to gain that much Flame Strength by cracking without coking is an important question to be determined! Finally, if the 160 1/s appears impractical or unworkable in the HiFIRE experiment, it is always possible to "ratchet up or down" the Flame Strength scale.

Comparison of Flame Strengths with Laminar Burning Velocities

Fig. 20 compares ASRs for the gaseous-HC extinction limits, from the 7.5 mm tube-OJB, with recently surveyed / published unstrained laminar burning velocity, $S_{L,0}$, measurements [56,57] at an equivalence ratio of unity (phi = 1). Fig. 21 extends the ASR results of Fig. 20 to include 100% H_2. Clearly, the ASRs reflect considerably more sensitivity to changes in fuel molecular size, type and reactivity than the $S_{L,0}$ data. In Fig. 20, a linear fit of the ASR vs $S_{L,0}$ data leads to a slope of 3.64, which appears inappropriately small for the (four lowest) saturated HCs. And in Fig. 21, a power-law fit of the gaseous-HC + H_2 data seems to represent the only available simple fit of the data. Whereas a power-law exponent of 1.87 fits the entire data set quite well, it also demonstrates a "strong apparent dependence" of ASR on a "relatively slowly changing" $S_{L,0}$. In conclusion, unstrained laminar burning velocity changes only *weakly* against highly strain-rate-sensitive Flame Strength variations. Thus, laminar burning velocity in premixed fuel + air is a relatively insensitive and probably unsatisfactory measure of fuel reactivity changes for use in assessing "idealized" strain-rate-sensitive flameholding at atmospheric pressure.

Experimental vs Numerical Extinction Limits, "Absolute" Axial Strain Rates

Since our early focus on methane + ethylene fuel mixtures [45], there have been at least three publications on numerically simulated extinction limits for nonpremixed CFDF flames, based on the respective components [59] and binary mixtures [60], and a contemporary numerical assessment of the chemical kinetic mechanism used to calculate both autoignition limits and extinction limits of mixtures in the present Conference [61]. Based on [59,60], our present ASR results in Fig. 6, and Eq. (2) developed earlier in this paper that enables the conversions of measured global ASRs from nozzle- and tube-OJBs to equivalent airside maximum axial strain rates, $(-du/dx)_{max}$, we now develop some "absolute" comparisons with the above numerically obtained values.

Fig. 22 shows a direct comparison, on an *absolute* airside maximum axial strain rate basis, of our averaged ASR extinction results for all the gaseous HCs shown in Figs. 9 and 10, with numerical results from Zambon & Chelliah [59], and Park & Fisher [60]. Before discussing the comparisons, it is important to note how the experimental ASR results and numerical results were plotted on the absolute-strain-rate scales of the ordinate and the abscissa. The empirical equation (Equation 2) for airside axial strain rate (shown in Fig. 22 for the ordinate) has been

derived in the paper. This enabled the plotting of all our experimental nozzle-OJB ASR_n results for gaseous HCs on the ordinate scale. The abscissa scale, which represents each experimental result for the respective gaseous HCs, was calculated from the expression on the abscissa label, which equals the second half of Eq. (2). Thus, in a similar fashion, the abscissa for each experimentally independent HC result was calculated from the ASR_t data.

Thus, the numerical simulation results plotted on the ordinate simply represent calculated airside maximum axial strain rates. However, the abscissa for each numerical result corresponding to each gas is (of necessity) the same as that used to plot each experimental "tube-OJB airside axial strain rate." Therefore the vertical separation between numerical axial strain rate and experimental ASR_n results represents an absolute discrepancy in airside maximum axial strain rate for each gas or gas mixture.

Inspection of Fig. 22 indicates that there is exceptionally good agreement between Zambron and Chelliah's methane extinction limit at 1 atm with our experimentally averaged result; this has been checked and reproduced repeatedly and semi-independently over the last 10 years [26]. The agreement with the Ref. 61 results for methane (not shown), using three recent kinetic models, appears to be similarly good. However, the numerical ethylene results from Refs. 59 and 60 are about 45% higher than the experimental result for ethylene, and the Ref. 61 results are respectively about 50%, 40%, and 30% high of the experimental result for ethylene. Due to the near-linear divergence of results from the methane "base," the predicted results for the 64% ethylene + 36% methane surrogate also appear to be about 45% high. Finally, the results of Park and Fisher [60] and Jiwen Liu [61] independently predict the observed experimental nonlinear FS response as a function of ethylene concentration.

Tests of Dynamic Flame Weakening of the 64/36 Ethylene/Methane Surrogate

The same basic 7.2 mm nozzle-OJB system used to measure (steady state) FSs and ASRs of gaseous HCs was previously used to characterize the Dynamic Flame Weakening (DFW) response of five gaseous HC-air systems [46-49]. For these measurements the twin speakers shown in Fig. 6a are driven at various pre-set amplitudes and frequencies to produce steady plus oscillatory velocity outputs at the nozzle exits, that push and pull in-phase. As the steady inflows are increased slowly, as with steady state flames, the resultant steady plus oscillatory inputs to these OJB flames cause sudden extinction in a manner similar to steady state extinction, except a flame will tend to rupture near the point of maximum "dome-like" extension (stretching) in the central region, as shown by video of the extinction events. Successively different voltage amplitudes are applied to the twin speakers at each frequency, and previously calibrated probe microphone data (@ 5 SLPM flows) are used to normalize the resultant sound pressure amplitudes, based on the applied voltage amplitudes. Finally the resultant DFW as each applied frequency is calculated as the percentage decrease in dynamic Flame Strength per pascal of peak-to-peak pressure oscillation (which parallels the velocity oscillation) [48,49].

Each fuel was characterized by (1) a steady-state FS (as before), (2) a unique quasi-steady DFW limit at low frequencies (say, 8, up to 15 or 20 Hz), (3) a systematically decreasing extent of DFW as frequencies approach 200 to 300 Hz, and finally (4) a regime where the flames become totally insensitive to oscillatory inputs (from 300 to 1600 Hz, the limit of the study), due to lagging diffusion response of the flame. Similar (proportional) DFW effects should be expected for tube OJBs.

Thus the same experimental system used previously to characterize the DFW of methane, ethane, propane, *n*-butane, and ethylene, was used in this study to characterize for the first time the DFW of the 64% ethylene / 36% methane surrogate proposed for use in Hi-FIRE, using the same procedures cited earlier [46-49]. Fig. 23 shows the resultant DFW characterizations as a function of applied frequency, along with similarly obtained results for pure methane and for three N_2-diluted ethylene mixtures and their averaged DFW results. The N_2-diluted ethylene mixtures (based on 3, 5, and 8 SLPM steady ethylene flows) extinguish under dynamic conditions at

respective mole fractions always greater than 0.38, 0.52, and 0.69, which apply for the respective maximum steady-state FSs (shown in Fig. A2).

In conclusion, the DFW results for the "64/36 surrogate" show that oscillations in OJB input flow velocity (and also fuel or air composition) may significantly weaken (extinguish) the 64/36 surrogate flames, up to 200 Hz. However, the surrogate flames are consistently weakened, about 2.5x less than for pure methane, and they are nearly as resistant to flow (and composition) oscillations as pure ethylene, which weakens about 5x less than methane.

GENERAL DISCUSSION

This paper describes the top-down methodology used to define simple gaseous surrogate hydrocarbon (HC) fuel mixtures for a hypersonic scramjet combustion subtask of the HiFIRE program. It then presents new and updated Opposed Jet Burner (OJB) extinction-limit Flame Strength (FS) data obtained from laminar non-premixed HC vs. air Counterflow Diffusion Flames at 1-atm, which follow from earlier investigations. FS represents a strain-induced extinction limit based on cross-section-average air jet velocity, U_{air}, that sustains combustion of a counter jet of gaseous fuel just before extinction. FS uniquely characterizes a kinetically limited fuel combustion rate. More generally, Applied Stress Rates (ASRs) at extinction (U_{air} normalized by nozzle or tube diameter, $D_{n\ or\ t}$) can be directly compared with extinction limits determined numerically using either a 1-D or preferably a 2-D Navier Stokes simulation with detailed transport and finite rate chemistry.

Flame Strength results for four binary gaseous HC systems, including two ternary gaseous systems and a ternary system with vaporized *n*-heptane, were obtained under idealized experimental conditions that allow comparisons with the results of detailed 1-D and 2-D numerical simulations, as global tests of proposed chemical kinetic models at 1-atm. The FS results help to characterize and define three candidate surrogate HC fuel mixtures that exhibit a common FS (ASR_t = 160 1/s) 70% greater than that for pure JP-7 fuel (93 1/s, which is equivalent to 15% ethylene + 85% methane). The candidates include a simple binary fuel mixture of 64% ethylene + 36% methane, which represents our primary recommendation. It is intended to mimic the critical flameholding limit of a thermally- or catalytically-cracked JP-7 "like" fuel in HiFIRE scramjet combustion tests.

The technical process of selectively defining and characterizing a simple gaseous hydrocarbon surrogate fuel, that will ignite and combust in a supersonic air stream for a HiFIRE test flight -- similar to a (hypothetical) cracked JP-7 "like" fuel in a scramjet combustor -- is discussed in detail. It is shown through a series of flowcharts that the extinction limits of non-premixed flames should be considered as the most representative for the primary initial ranking of strain-rate-limited combustion rates in the highly strained flameholding regions of a cavity flameholder.

The paper reviews a recent summary (Ref. 45) of the normalization of FSs of pure and N_2-diluted fuel systems to account for the effects of temperature, pressure, jet diameter, inflow Reynolds number, inflow velocity profile (plug from contoured nozzle; parabolic from straight tube) and fuel composition. It is concluded that "Through comparisons with earlier OJB characterizations, normalized (ASR) results exemplify a sensitive accurate means of validating, globally, complete and reduced chemical kinetic models at the relatively low temperatures that govern the loss of non-premixed "idealized" flameholding at near-atmospheric pressure, e.g., in scramjet combustors."

The new experimental ASR results refine the "idealized flameholding dual-reactivity scale" (Ref. 45) that shows wide ranging (50 x) ASRs at extinction, for respective plug and parabolic inflows, using various undiluted vaporized-liquid and gaseous HCs. These now include, in ascending order: JP-10, methane, JP-7, *n*-butane, *n*-heptane, propane, propylene, *n*-dodecane, ethane, the 64% ethylene / 36% methane surrogate, and ethylene. Additional results from H_2–air

produce a unique and exceptionally strong flame that agree within about 1% of a recent 2-D numerically simulated FS for a 3 mm tube-OJB.

Recent numerical extinction results for methane, ostensibly based on the best available validated chemical kinetics for HCs, agree quite closely (within ~10%) with the measured ASRs, that are translated to an absolute strain rate scale. Thus we suggest that experimental ASRs for various neat and blended HCs with and without additives, offer accurate global tests for chemical kinetic models at the temperatures and pressures of extinction.

CONCLUDING REMARKS

The new and updated OJB laminar FS (ASR) results are summarized and concluded as follows:

(1) The refined exit-diameter-normalized-FS, or Applied Stress Rate (ASR) dual-reactivity scale, based on respective convergent nozzle- and tube-OJB extinction results, provides a sensitive and potentially accurate representation of “maximum strength” non-premixed pure-HC vs air flames at 1-atm, for gaseous and vaporized liquid fuels.

(2) ASR “scaling” is recommended as a straightforward and sensitive means of provisionally ranking HC fuels for “minimal” scramjet flameholding in much more complex subsonic recirculation flow fields.

(3) The present FS characterizations use, as a starting point, a ternary surrogate fuel of 60% ethylene + 30% methane + 10% *n*-heptane, which Colket and Spadaccini (2001) proposed (based on substantial published and unpublished data) to match the ignition delay of a “typical” cracked JP fuel.

(4) The FS data analyses show how our recommended binary “64/36” gaseous surrogate (64% ethylene + 36% methane) has an ASR_t (160 1/s) identical to that of Colket and Spadaccini’s ternary surrogate, and 70% higher than that for vaporized un-cracked JP-7 (93 1/s, which is equivalent to 15% ethylene + 85% methane). Note the H/C ratio of our “64/36” surrogate (2.44) differs from that for Colket’s ternary surrogate (2.36) or JP-8 (1.91), and the H/C ratio does affect the relative heat release and H_2O / CO_2 ratio of exhaust products and thrust performance of a fuel.

(5) Identical ASRs (160 1/s) also characterize an alternate surrogate of 44% ethylene + 56% ethane. Its components have nearly equal molecular weights and roughly similar HC ratio (2.56), which may be useful if fuel composition is varied systematically in a series of scramjet combustion tests. However, this surrogate mixture liquefies at much lower pressure, which limits on-board storage of *gaseous* fuel.

(6) Dynamic Flame Weakening results show how oscillations in OJB input flow velocity (and also fuel or air composition) may significantly weaken (extinguish) 64/36 surrogate flames up to 200 Hz. However, they are weakened about 2.5x less than methane alone, and are nearly as resistant to flow (and composition) oscillations as ethylene, which weakens about 5x less than methane.

(7) ASR limits at 1-atm are compared on an absolute maximum airside-input axial strain rate scale (formalized in this paper) with three recently published 1-D numerical OJB extinction limits (FSs) for non-premixed HC–air systems. The methane chemical kinetic models agree quite closely, whereas, the three independently predicted FSs, using three slightly different contemporary ethylene kinetics models, predict FSs that are ~ 45% high. This represents a significant problem for numerical simulation of surrogate-based combustion simulations in a scramjet flameholding cavity.

The Flame Strength approach is advocated as a more fundamental and meaningful measurement, for assessing idealized scramjet flameholding potentials, than laminar burning velocity or blowout in a Perfectly Stirred Reactor. This is because the latter characterize premixed combustion in the absence of aerodynamic strain, and FS *directly* measures a chemical-kinetic-controlled strain-rate-sensitive limit of non-premixed combustion at typical incipient-flameholding temperatures. Thus it approximately mimics an idealization of conditions where gaseous fuels are injected (and transported from upstream injection) into a subsonic flameholding recirculation zone. Here, air captured from the upstream inlet and overriding flow mixes and reacts with the fuel, and the effects of local aerodynamic strain and associated multi-component diffusion on incipient flameholding-combustion are still operative.

Finally, we continue advocating that a remotely operated OJB system be considered to achieve real-time (e.g., 1 minute) characterizations of the idealized flameholding potential (ASR) of high-T, high-pressure, multi-component, vaporized and partially cracked hydrocarbon fuels being used for scramjet testing. This is driven by the likelihood of wide variations in fuel composition from test to test. Independent OJB extinction data should also be obtained and compared with other reference sources of vaporized and cracked HCs, e.g., fuels processed by idealized bench-top vaporizer / catalytic cracking systems, or fuels captured by "freezing" the composition of cracked vaporized (superfluid) HCs from other prototype heater / vaporizer / catalytic-cracking systems. Thus, we suggest that measurements of FS could be, and probably should be, a key routine HC fuel characterization parameter for any scramjet combustor test. Similar logic may be applied to the development of any complex surrogate HC fuel mixture, such that its measured FS mimics that of a typical uncracked- or cracked fuel, and, in principle, its FS can be numerically simulated using available chemical kinetics and a detailed OJB code.

ACKNOWLEDGEMENTS

The authors gratefully acknowledge the experimental and analytical assistance of Ms. Rachel Burke and Mr. Merritt Boyd, both NASA Virginia Governor's School students, during their four-week summer-of-2007 tenure at the NASA Langley Research Center.

REFERENCES

1. Spadaccini, L.J., "Autoignition "Characteristics of Hydrocarbon Fuels at Elevated Temperatures and Pressures," ASME Paper No. 76-GT-3, March, 1976, 5 pp.

2. Spadaccini, L.J., and TeVelde, J.A., "Autoignition Characteristics of Aircraft-Type Fuels," *Combust. Flame* **46**, (1982), pp. 283-300.

3. Edwards, T., "USAF Supercritical Hydrocarbon Fuels Interests," AIAA Paper 93-0807, Jan., 1993, 11 pp.

4. Maurice, L.Q., Corporan, E., Minus, D., Mantz, R., Edwards, T., Wohlwend, K. Harrison, W.E., Striebich, R.C., Sidhu, S. Graham, J., Hitch, B., Wickham, D, and Karpuk, M., "Smart Fuels: "Controlled Chemically Reacting Fuels," AIAA Paper AIAA 99-4916, July, 1999, 11 pp.

5. Wickham, D.T., Alptekin, G.O., Engel, J.R., and Karpuk, M.E., "Additives to Reduce Coking in Endothermic Heat Exchangers," AIAA Paper AIAA 99-2215, July, 1999, 9 pp.

6. Colket, M.B., III, and Spadaccini, L.J., "Scramjet Fuels Autoignition Study," J. Propulsion and Power, **17**, No. 2, 2001, Mar.-Apr. 2001, pp. 315-323.

7. Gruber, M. Dunbar, J., and Jackson, K., "Newly Developed Direct-Connect High- Enthalpy Supersonic Combustion Research Facility," J. Propulsion and Power, **17**, No. 6, Nov.-Dec. 2001, pp. 1296-1304.

8. Mathur, T., Gruber, M., Jackson, K., Donbar, J., Donaldson, W., Jackson, T., and Billig. F., "Supersonic Combustion Experiments with a Cavity-Based Fuel Injector," J. Propulsion and Power, **17**, No. 6, Nov.-Dec. 2001, pp. 1305-1312.

9. Quick, A., King, P.I., Gruber, M.R., Carter, C.D., and Hsu, K-Y., "Upstream Mixing Cavity Coupled with a Downstream Flameholding Cavity Behavior in Supersonic Flow," AIAA Paper AIAA-2005-3709, July, 2005, 13 pp.

10. Rasmussen, C.C., Driscoll, J.F., Hsu, Kuang-Yu, Donbar, J.M., Gruber, M.R., and Carer, C.D., "Stability Limits of Cavity-Stabilized flames in Supersonic Flow," Proceedings of the Combustion Institute **30** (2005), pp. 2825-2833.

11. Cooke, J.A., Bellucci, M., Smooke, M.d., Gomez, A., Violi, A., Faravelli, T. and Ranzi, E., "Computational and Experimental Study of JP-8, a Surrogate, and its Components in Counterflow Diffusion Flames," Proceedings of the Combustion Institute **30** (2005), pp. 439-446.

12. Maurice, L.Q, Edwards, T., Cuoco, F. Bruno, C, and Hendrick, P., CHAPTER 2: Fuels, in *Technologies for Propelled Hypersonic Flight*, RTO-TR-AVT-007, Volume 2 – Subgroup 2: Scram Propulsion, ISBNs 978-92-837-0041-4 / 978-92-837-0041-8, Jan. 2006, pp. 2-1 through 2-35.

13. Liu, Jiwen, Tam, C-J, Lu, T., and Law, C.K., "Simulations of Cavity-Stabilized Flames in Supersonic Flows Using Reduced Chemical Kinetic Mechanisms," AIAA Paper 2006-4862, 42nd AIAA Joint Propulsion Conf., 9-12 July 2006, 15 pp.

14. Humer, S., Frassoldati, A., Granata, S., Faravelli, T., Ranzi, E., Seiser, R., Seshadri, K., "Experimental and kinetic modeling study of combustion of JP-8, its surrogates and reference components," Proceedings of the Combustion Institute, **31** (2007), pp. 393-400.

15. Holley, A.T., Dong, Y., Andac, M.G., Egolfopoulos, F.N., Edwards, T., "Ignition and extinction of non-premixed flames of single-component liquid hydrocarbons, Jet fuels, and their surrogates," Proceedings of the Combustion Institute, **31**, 2007, pp. 1205-1213.

16. Allen, W., King, P.I., Gruber, M.R., Carter, C.D., and Hsu, K-Y, "Fuel-Air Injection Effects On Combustion In Cavity-Based Flameholders In a Supersonic Flow," AIAA Paper 2005-4105, 41st AIAA Joint Propulsion Conf., 10-13 July, 2005, 12 pp.

17. Lin, K-C, Tam, C-J, Boxx, I., Campbell, C, Jackson, K., and Lindsey, M., "Flame Characteristics and Fuel Entrainent Inside a Cavity flame Holder in a Scramjet Combustor," AIAA Paper 2007-5381, 43rd AIAA Joint Propulsion Conf., 8-12 July, 2007, 19 pp.

18. Lin, K-C, Jackson, K., Behdadnia, R., Jackson, T.A., Ma, F. Li, J., and Yang, V., "Acoustic Characterization of an Ethylene-Fueled Scramjet Combustor with a Recessed Cavity flameholder," AIAA Paper 2007-5382, 43rd AIAA Joint Propulsion Conf., 8-12 July, 2007, 11 pp.

19. Montgomery, C.J., Tang, Q., Sarofim, A.F., Bozzelli, J.W., "Supersonic Reacting Flow Simulations Using Reduced Chemical Kinetic Mechanisms and Multiprocessor ISAT," Paper AIAA 2008-1014, 46th AIAA Aerospace Sciences Meeting, 7-10 Jan., 2008, 10 pp.

20. Colket, M. Edwards, T, Williams, S, Cernansky, N.P., Miller, D.L., Egolfopoulos, F., Lindstedt, P., Seshadri, K., Dryer, F.L., Law, C.K., Friend, D, Lenert, D.B., Pitsch, H., Sarofim, A., Smooike, M., and Tsang, W., "Development of an Experimental Database and Kinetic Models for Surrogate Jet Fuels," Paper AIAA-2007-770, 45th AIAA Aerospace Sciences Meeting, 8-11 Jan., 2007, 21 pp.

21. Hongzhi, R. Zhang, Eddings, E. G., Sarofim, A.F., “Criteria for selection of components for surrogates of natural gas and transportation fuels,” Proceedings of the Combustion Institute, **31** (2007), pp. 401-409.

22. Valorani, M., Creta, F., Donato, F., Najm, H.N., Goussis, D.A., “Skeletal mechanism generation and analysis for *n*-heptane with CSP,” Proceedings of the Combustion Institute, **31** (2007), pp. 483-490.

23. Liu, S., Hewson, J.C., Chen, J.H., “Nonpremixed *n*-heptane autoignition in unsteady counterflow,” *Combust. Flame* **145**, (2006), pp. 730-739

24. Holley, A.T., Dong, Y., Andac, M.G., Egolfopoulos, F.N., “Extinction of premixed flames of practical liquid fuels: Experiments and simulations,” *Combust. Flame* **144**, (2006), pp. 448-460.

25. Andac, M.G. and Egolfopoulos, F.N., “Diffusion and kinetics effects on the ignition of premixed and non-premixed flames,” Proceedings of the Combustion Institute, **31** (2007), pp. 1165-1172.

26. Pellett, G.L., Isaac, K.M., Humphreys, W.M., Jr., Gartrell, L.R., Roberts, W.L., Dancey, C.L., and Northam, G.B., "Velocity and Thermal Structure, and Strain-Induced Extinction of 14 to 100% Hydrogen-Air Counterflow Diffusion Flames," *Combust. Flame* **112**, No. 4, 1998, pp. 575-592.

27. Pellett, G.L., Northam, G.B., Guerra, R., and Wilson, L.G., “Opposed Jet Burner Studies of Silane-Methane, Silane-Hydrogen, and Hydrogen Diffusion Flames with Air,” CPIA Publication 457, Vol. 1, Oct. 1986, pp. 391-404.

28. Pellett, G.L., Northam, G.B., Wilson, L.G., Jarrett, O., Jr., Antcliff, R.R., Dancey, C.L., and Wang, J.A., "Opposed Jet Diffusion Flames of Nitrogen-Diluted Hydrogen vs. Air: Axial LDA and CARS Surveys; Fuel/Air Strain Rates at Extinction," AIAA Paper 89-2522, July 1989, 19 pp.

29. Guerra, Rosemary, Pellett, G.L., Wilson, L.G., Northam, G.B., "Opposed Jet Burner Studies of Hydrogen Combustion with Pure and N_2, NO Contaminated Air," AIAA Paper 87-0090, Jan. 1987, 11 pp.

30. Guerra, Rosemary, Pellett, G.L., Wilson, L.G., Northam, G.B., "Opposed Jet Burner Studies of Effects of CO, CO_2 and N_2 Air Contaminants on Hydrogen-Air Diffusion Flames," AIAA Paper 87-1960, July 1987, 14 pp.

31. Pellett, G.L., Jentzen, M.E., Wilson, L.G., and Northam, G.B., "Effects of Water-Contaminated Air on Blowoff Limits of Opposed Jet Hydrogen-Air Diffusion Flames," AIAA Paper 88-3295, July 1988, 10 pp.

32. Pellett, G.L., Wilson, L.G., Northam, G.B., Guerra, Rosemary, "Effects of H_2O, CO_2, and N_2 Air Contaminants on Critical Airside Strain Rates for Extinction of Hydrogen–Air Counterflow Diffusion Flames," CPIA Publication 529, Vol. II, (Oct., 1989), pp. 23-42. Pasadena, CA, Oct., 1989.

33. Pellett, G.L., Northam, G.B., Wilson, L.G., "Counterflow Diffusion Flames of Hydrogen, and Hydrogen Plus Methane, Ethylene, Propane, and Silane, vs. Air: Strain Rates at Extinction," AIAA Paper 91-0370, Jan., 1991, 17 pp.

34. Pellett, G.L., Northam, G.B., Wilson, L.G., "Strain-Induced Extinction of Hydrogen–Air Counterflow Diffusion Flames: Effects of Steam, CO_2, N_2, and O_2 Additives to Air," AIAA Paper 92-0877, Jan., 1992, 15 pp. (Also a manuscript in preparation on these and recent 2-D numerical results.)

35. Pellett, G. L., Roberts, W. L., Wilson, L. G., Humphreys, W. M., Jr., Bartram, S. M., Weinstein, L. M., and Isaac, K. M., "Structure of Hydrogen–Air Counterflow Diffusion Flames Obtained by Focusing Schlieren, Shadowgraph, PIV, Thermometry, and Computation,” AIAA Paper 94-2300, June 1994, 23 pp.

36. Pellett, G. L., Wilson, L. G., Humphreys, W. M.,Jr., Bartram, S. M., Gartrell, L. R., and Isaac, K. M., Roberts, W. L., IV, and Northam, G. B., "Velocity Fields of Axisymmetric Hydrogen-Air Counterflow Diffusion Flames from LDV, PIV, and Numerical Computation," AIAA paper 95-3112, July 1995, 23 pp.

37. Isaac, K. M., Ho, Y. H., Zhao, J., Pellett, G. L., and Northam, G. B., "Global Characteristics and Structure of Hydrogen-Air Counterflow Diffusion Flames: A One-Dimensional Model," AIAA Paper 94-0680, Jan.,1994. Also, Zhao, J., Isaac, K. M., and Pellett, G. L., *J. Propul. Power* **12**, No. 3 (1996), pp. 534-542.

38. Pellett, G.L., Isaac, K.M., and Nguyen, G., "Effect of Input Temperature on Strain-Induced Extinction of 50 to 100% Hydrogen–Air Counterflow Diffusion Flames," Presented at 27th Symposium (International) on Combustion, Abstracts of Work-In-Progress Poster Presentations, The Combustion Institute, Pittsburgh, PA, Poster W2D01, Aug., 1998, p. 192.

39. Pellett, G.L., Bruno, C., and Chinitz, W., "Review of Air Vitiation Effects on Scramjet Ignition and Flameholding Combustion Processes," AIAA Paper 2002-3880, July 2002, 37 pp.

40. Pellett, G.L., Bruno, C, and Chinitz, W., CHAPTER 4: Air Vitiation Effects on Scramjet Combustion Tests, in *Technologies for Propelled Hypersonic Flight*, RTO-TR-AVT-007, Volume 2 – Subgroup 4: Scram Propulsion, ISBNs 978-92-837-0041-4 / 978-92-837-0041-8, Jan. 2006, pp. 4-1 - 4-21.

41. Hwang, Kyu C., "Two Dimensional Numerical Simulation of Highly-Srained Hydrogen–Air Opposed Jet Laminar Diffusion Flames," Ph. D. Dissertation, Old Dominion University, Norfolk, VA, May 2003.

42. Convery, J.L., Pellett, G.L., O' Brien, W.F., and Wilson, L.G., "An Experimental Study of *n*-Heptane and JP-7 Extinction Limits in an Opposed Jet Burner," AIAA Paper 2005-3766, July 2005, 8 pp.

43. Convery, J.L., "An Experimental Investigation of JP-7 and *n*-Heptane Extinction Limits in an Opposed Jet Burner," MS Thesis in Mechanical Engineering, Virginia Polytechnic Institute and State University, Blacksburg, VA, October 27, 2005, 52 pp.

44. Pellett, G.L., Convery, J.L, Wilson, L.G., "Opposed Jet Burner Approach for Characterizing Flameholding Potentials of Hydrocarbon Scramjet Fuels," AIAA Paper 2006-5233, July 2006, 27 pp.

45. Pellett, G.L., Vaden, S.N., and Wilson, L.G., "Opposed Jet Burner Extinction Limits: Simple Mixed Hydrocarbon Scramjet Fuels vs Air," AIAA Paper 2007-5664, July 2007, 33 pp.

46. Pellett, G.L., Reid, Beth, McNamara, Clare, Johnson, Rachel, Kabaria, Amy, Panigrahi, Babita, and Wilson, L.G., "Acoustic Weakening of Methane-, Ethylene-, and Hydrogen-Air Counterflow Diffusion Flames, and Implications for Scramjet Flameholding." AIAA Paper 2003-4634, July 2003, 21 pp.

47. Pellett, G., Reid, B., McNamara, C., Johnson, R., Kabaria, A., Panigrahi, B., Sammons, K., and Wilson, L., "Dynamic Weakening of CH_4–, C_2H_6–, and C_2H_4/N_2–Air Counterflow Diffusion Flames using Acoustically Perturbed Inflows." Work-in-Progress Poster Paper 4F504, Presented at 30th International Symposium on Combustion, Abstracts of Work-In-Progress Posters, The Combustion Institute, Pittsburgh, PA, July 25-30, 2004.

48. Pellett, G.L., Kabaria, A., Panigrahi, B., Sammons, K., Convery, J., and Wilson, L.G., "Dynamic Weakening (Extinction) of Simple Hydrocarbon–Air Counterflow Diffusion Flames by Oscillatory Inflows." AIAA Paper 2005-4332, July 2005, 22 pp.

49. Pellett, G.L, McNamara, C., Johnson, R., Kabaria, A., Panigrahi, B., Sammons, K., Galgano, J., and Wilson, L.G., "Dynamic Weakening of Gaseous Hydrocarbon (C1-C4)–Air Counterflow Diffusion

Flames by Oscillatory Inflows," Work-in-Progress Poster Paper 4B01, Presented at 31st International Symposium on Combustion, Abstracts of Work-In-Progress Poster Presentations, The Combustion Institute, Pittsburgh, PA, Aug. 6-11, 2006.

50. Guthhel, E., and Williams, F., 23rd *Symposium (International) on Combustion*, The Combustion Institute, Pittsburgh, 1990, p. 513.

51. Guthhel, E., Balakrishnan, G., and Williams, F., in *Reduced Kinetic Mechanisms for Application in Combustion Systems*, Lecture Notes in Physics (N. Peters and B. Rogg, eds.) Springer-Verlag, New York, 1992, p. 177.

52. Rolon, J.C., Veynante, D., Martin, J.P., and Durst, E., "Counter Jet Stagnation Flows," Experiments in Fluids, **11**, 1991, pp. 313-324.

53. Spalding, D.B., "Theory of Mixing and Chemical Reaction in the Opposed-Jet Diffusion Flame," *J. Amer. Rocket Soc*., **3**, 1961, pp. 763-771.

54. Williams, F.A., "A Review of Flame Extinction," *Fire Safety J.*, **3**, 1981, pp. 163-175.

55. Seiser, R., Truett, L., Trees, D., and Seshadri, K., "Structure and Extinction of Non-premixed *n*-Heptane Flames," 27th Symposium (International) on Combustion, The Combustion Institute (1998), pp. 649-657.

56. Hassan, M.I., Aung, K.T., Kwon, O.C., and Faeth, G.M., "Properties of Laminar Premixed Hydrocarbon / Air Flames at Various Pressures," *J. Propulsion and Power*, **14**, No. 4, 1998, pp. 479-488.

57. Bosschaart, K.J., and de Goey, L.P.H., "The Laminar Burning Velocity of Flames Propagating in Mixtures of Hydrocarbons and Air Measured with the Heat Flux Method," *Combustion and Flame*, **136**, 2004, pp. 261-269.

58. Ciani, Andrea, "Hydrogen and Methane Edge and Diffusion Flames in Opposed Jet Configurations: Structure and Stability." Dissertation, submitted to the Swiss Federal Institute of Technology Zurich, Switzerland, for the degree of Doctor of Technical Sciences, Doctoral Thesis ETH No. 16540, 2006, 108 pp.

59. Zambon, A.C, Chelliah, H.K., "Explicit reduced reaction models for ignition, flame propagation, and extinction of $C_2H_4/CH_4/H_2$ and air systems," Combust. Flame (2007), in press, doi 10 1016/I combustflame 2007 03 003.

60. Park, Okjoo, and Fisher, E.M., "Calculated extinction strain rates for binary fuel mixtures," Paper No. B-27, Eastern States Fall Technical Meeting of the Combustion Institute, U. of Virginia, Charlottesville, Va., Oct. 21-25, 2007.

61. Liu, Jiwen, Eklund, D., and Gruber, M., "Chemical Kinetic Mechanism Validation for Combustion of Mixture Fuel of Methane and Ethylene," Paper for presentation at the 55th JANNAF Propulsion Meeting, May 12-16, 2008, Boston, MA.

62. Dattarajan, S., Montgomery, C.J., Gouldin, F.C., Fisher, E.M., Bozzelli, J.W., "Extinction of Opposed Jet Diffusion Flames of Scramjet Fuel Components at Subatmospheric Pressures," AIAA Paper 2008-996, 46th AIAA Aerospace Sciences Meeting, 7-10 Jan., 2008, 9 pp.

APPENDIX A – SUPPORTING STRAIN RATE CHARACTERIZATIONS

Measured and Estimated Strain Rates for Cold and Hot Opposed Flows

(**1**) Fig. A1 shows our earlier comparisons [44] of Rolon's Laser Doppler Anemometry (LDA-measured strain rates (SRs), for varying separations of twin 25 mm contoured nozzles, and fixed flows of air vs air with balanced axial jet momentum flux [52]. Both the measured radial SR, and – 1/2 the measured axial SR are shown as a function of nozzle separation, H. In addition, Spalding's suggested approximation in 1961 [53] for the radial SR is shown for very large uniform impinging flows, i.e., U_{air}/D_n. Note this approximation has been used by the present authors for some time to represent ASR for convergent nozzles [26,33,37,44], and it is only ~ 15% lower than Rolon's measured SRs at $H/D \geq 1$. However, the $2U_{air}/H$ approximation, developed in [54], is based on an assumed linear axial velocity gradient, and balanced axial momentum fluxes for cold flows from large matrix type OJBs (typically 22 mm diameter), and produces a SR that is *excessively large* under typical operating conditions (H/D ~ 0.45). The present authors found the reported SRs from the matrix burner too high by a factor of ~ 1/0.42 (= 2.4), to match (with a short extrapolation) Rolon's measured radial SR (45 1/s) for nozzle-OJB flows. As pointed out by Rolon et. al [52], the $2U_{air}/H$ approximation only converges on the measured -1/2 axial and radial SRs beyond $H/D > 1$, preferably ≥ 1.5. In our subsequent analyses (main body of paper) of tube-OJB data [42-44], and comparison with published *n*-heptane/N_2–air extinction data from a 22 mm matrix burner [55] and *n*-dodecane–air using the same apparatus [14], we first applied the above correction factor of 1/0.42 to allow for a SR data comparison with nozzle-OJB flows. Then a further factor of 2.5 was applied to tube-OJB results for hot vaporized hydrocarbons, to convert them to equivalent nozzle-OJB results.

(**2**) The author's previous extensive ASR extinction results, for N_2-diluted H_2 vs air using tube-OJBs with parabolic inflows [26] ($ASR_t = U_{air}/D_t$), were well characterized for wide-ranging tube diameters (1.8 - 10 mm) and H_2 concentrations (20 - 100%) [45]. However, these H_2/N_2–air ASR extinction data were found to differ systematically from the entire set of HC–air ASR data from both nozzle-OJBs with plug inflows and tube-OJBs with parabolic inflows [45]. An updated plot, shown in Fig. A3, contains all the present gaseous HC results. It shows the ASR_n / ASR_t ratio for seven pure HCs at extinction is always ~ 2.2, whereas the same ASR ratio varies between 4 and 2.7 for H_2 inputs ranging 14 to 100%.

The large difference in ASR ratios at extinction primarily reflects significantly different molecular diffusion rates on the airside (and also lower flammability limits) for H_2 in air, which cause significant differences in the offsets of the airside CFDF from the stagnation point (greater for H_2) for respective nozzles and tubes. Thus the maximum radial strain rate experienced by the H_2–air flame core is reduced somewhat, relative to what it would be (at the same ASR inflow) if the flame were closer to the stagnation point. This in turn requires a larger ASR to achieve extinction. And because the rate of diffusion of many HC species is generally much lower than for H_2, airside HC flames locate significantly closer to the stagnation point, where radial SRs are larger and closer to being ideal for 1-D models [26]. As a result, the ASR extinction ratios for all seven of the present gaseous HCs are clustered at a lower ratio near 2.2, which is much closer to Hwang's [41] numerically simulated values of 2.5 for both cold and hot parabolic / plug inflows.

In other words, because the divergence of an OJB air jet increases systematically as the stagnation point is approached, the local radial strain rate that effectively controls extinction also varies with the axial flame offset (and the inflow profile), and reaches a maximum at the SP [41]. As a consequence of the various H_2 flames always being located significantly further upstream from the SP than HC flames, in respective plug and parabolic inflow cases, the measured ASR_n / ASR_t ratio for H_2 flames at extinction is always uniquely higher, and is also a moderate function of N_2 dilution.

(**3**) Two master plots of extinction limits for five previously studied simple gaseous HC-air systems, with several OJB tube sizes used (7 sets, 2.7 – 10 mm), illustrate *asymptotic* approaches towards effectively constant ASR_t extinction limits for each fuel *as tube diameter increases* (relative to flame thickness), *and as exit Reynolds number increases*, but remains below 2000 [44,45].

(**4**) Fig. A2 shows FSs for N_2-diluted ethylene–air systems, obtained using a 7.2 mm vertical "flowfield-standardized" contoured-Pyrex nozzle-OJB with 14 mm spacing. For this system, an asymptotic FS value for 100% C_2H_4 was estimated (projected), because the FS of ethylene was so high that the fuel mass flow meter just exceeded its operational limit. This same system was used for all the nozzle-OJB extinction characterizations in this study (total of seven gaseous HCs).

(**5**) The same 7.2 mm nozzle-OJB system was also used for nozzle-OJB dynamic FS measurements to characterize the dynamic response of five gaseous HC-air systems [46-49]. Thus steady plus oscillatory velocity inputs caused unique and systematically decreasing extents of Dynamic Flame Weakening (for each fuel), at frequencies from 8 to > 200 Hz. Notably, from 300 to 1600 Hz (limit of the study), further weakening due to lagging diffusion response of the flame was negligible in every case, as flames became totally insensitive to oscillatory inputs. Similar (proportional) DFW effects should be expected for tube OJBs. The same system was used in the present study to characterize, for the first time, the dynamic response of the 64% ethylene/36% methane surrogate proposed for use in Hi-FIRE (see Fig. 23).

(**6**) Notably, extinction limits for *all* the N_2-diluted H_2 and HC systems investigated showed *asymptotic approaches to nearly constant FSs* as pure fuel was approached (unity mole fraction of combustible), using both plug-inflow nozzle- and parabolic-inflow tube-OJBs. Thus extinction limits are essentially *unaffected* by increasing fuel diffusion rates (with increasing fuel mole fraction) to the (generally) airside flames, and hence extinctions of pure fuel are controlled primarily by chemical kinetic rates, as in the H_2 systems.

(**7**) The FSs of N_2-diluted vaporized *n*-heptane and JP-7 mixtures vs air also exhibited the same kinetically limited (asymptotic) behavior, as did the normally gaseous HCs. In addition, these *n*-heptane data compared favorably with published extinction results (available up to a 26 mole % limit), *when the published data from* relatively *small gaps were appropriately corrected* [44,45], based on Rolon's LDA strain rate characterizations [52] described in Fig. 1A. New experimental FS data on 100% *n*-dodecane and 50/50 molar mixture of *n*-heptane + *n*-dodecane are shown in the present paper along with our analysis of newly published extinction data on (heavily) N_2-diluted *n*-dodecane using the same data corrections.

(**8**) A series of four figures illustrate the strong negative effects on FSs of using methane, propane, and ethylene HCs to dilute H_2 (and "scavenge" H-atoms), compared to the negligible effects of N_2 dilution on FSs at high H_2 concentrations (say, 80% – 100%) [44]. These plots also show essentially negligible effects on FS of H_2 addition to HCs, say up to 20% H_2. This finding is qualitatively consistent with Colket & Spadaccini ignition data [6] that showed similarly no effect of significant H_2 addition.

In summary of the above, Refs. [42-44], and especially [45], provide extensive fundamental OJB extinction data and analyses that help to better define the effects of air and (especially) fuel input temperature, barometric pressure and jet diameter, and inflow Reynolds number and velocity profile (plug vs parabolic inflows) on FSs and ASRs, for the global testing of detailed chemical kinetic models for HC fuels. They also produce a refined characterization of "idealized flameholding potentials" that apply over a very wide-ranging scale of kinetically limited fuel reactivity (extinction limits) caused by highly strained aerodynamic flows under well-defined conditions. Thus the FS and ASR approach that helps define "incipient" flameholding limits in simple and practical HC-air systems at ~ 1 atm is also considered a useful and convenient basis for assessing the loss of non-premixed idealized, incipient flameholding in more complex scramjet combustors.

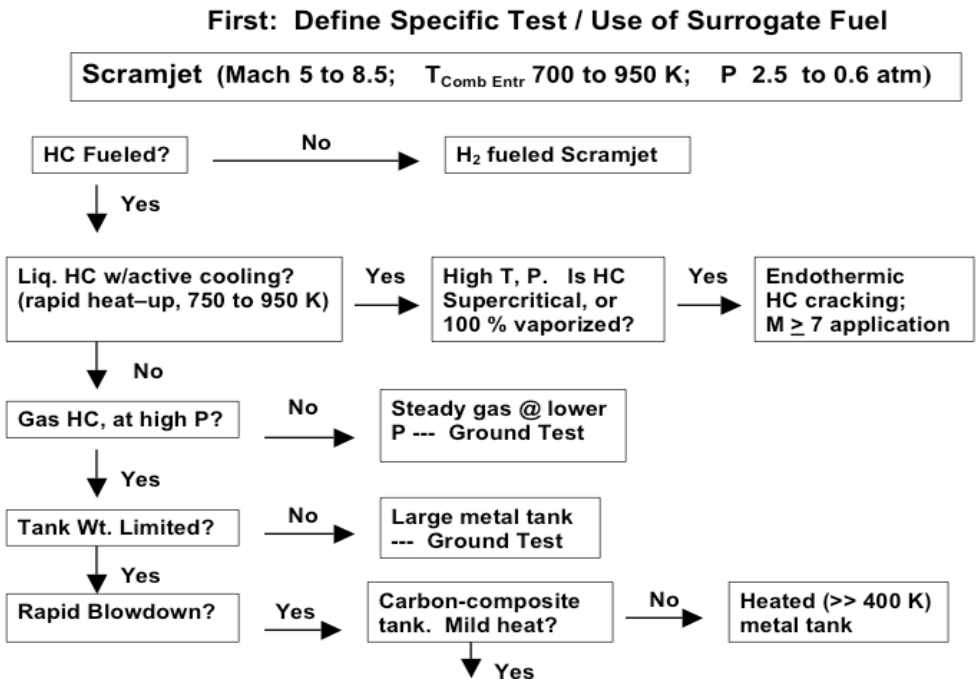

Fig. 1. Flow chart view of the process of defining specific tests and uses of generic HC surrogate fuels that might power a scramjet to Mach 8, with application to the present subtask of the HiFIRE program

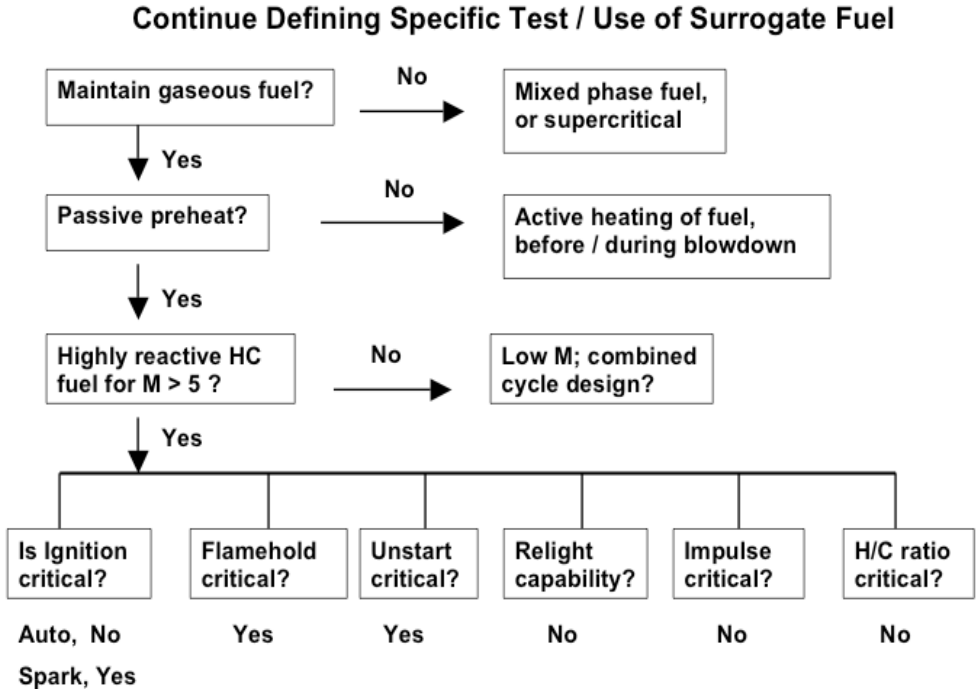

Fig. 2. Continue flow chart view of the process of defining specific tests and uses of generic HC surrogate fuels for the present subtask of the HiFIRE program. “Flameholding” is considered critical along with “spark ignition” and “unstart.”

Target Bases for Surrogate Fuels – AFTER Use is Specified

Fuel Properties:

Chemical composition profile; Energy density; Density; Viscosity.

C/H ratio (determines Fuel / Air mass flow ratio).

Liquid/Vapor partitioning; Evaporation-Condensation; Subcritical Inj.

Relative to Engine Design / Characteristics:

Auto-ignition; Spark-induced ignition; Relight.

Flameholding – Too robust (Unstart); Robust; Weak; Blowout.

Heat-release-rate profile & magnitude; Performance prediction.

Emissions – HC, CO, NO_x, Soot.

Fig. 3a. Delineation of a comprehensive set of "target bases for surrogate fuels" *after* the primary use has been specified." Fuel properties are dominated by the need to retain the vapor state at all times. Flameholding is the most important relative to engine design / characteristics.

Target Bases for Surrogate Fuels (concluded)

Laboratory studies of Premixed fuels / flames –-- Shock Tube and Sphere (ignition); Perfectly Stirred Reactor; Flow Reactor; Dual-flame OJB.

Non-Premixed --- Jet Diffusion Flames; Counter-Flow OJB:

***Premixed* flame Properties:**

Auto-ignition delay. Critical ignition energy / kernel. Lam. Flame Speed.
Extinction Limits (Phi, P, T_o): Twin, or lean / rich dual-flame.
T, composition profiles; product evolution rates.
Sooting characteristics.

***Non-Premixed* flames:**

Auto-ignition delay. Extinction Limits (P, T_o)

Composition, T profiles; and combustion / evolution rates.

Sooting characteristics.

Fig. 3b. Continue delineation of "target bases for surrogate fuels *after* the primary use has been specified." Note that "Counter-Flow OJB" is selected for application to determine extinction limits of non-premixed flames for this study.

Functional Comparisons, Scramjet- with Opposed-Jet-Flameholding

Characteristic of Flameholding	Scramjet w/ Cracked JP-7	OJB w/ Gas Surrogate
Gaseous fuel	Yes	Yes
Non-premixed Combustion	Yes	Yes
Laminar Flamelet (e.g., Large Eddy diff.)	Yes	Yes
Cause of Extinction		
High strain rate sensitivity	Yes	Yes
Fuel/Air Composition sensitivity	Yes	Yes
Sensitivity to dynamic fluctuations	Yes	Yes
Auto-Ignition delay matching (Colket)	Yes	Yes

Fig. 4. Definition of some of the “functional comparisons” and distinctions between Scramjet flameholding with a hypothetical cracked JP-7 “like” fuel and the present OJB experimental approach to “idealized flameholding.”

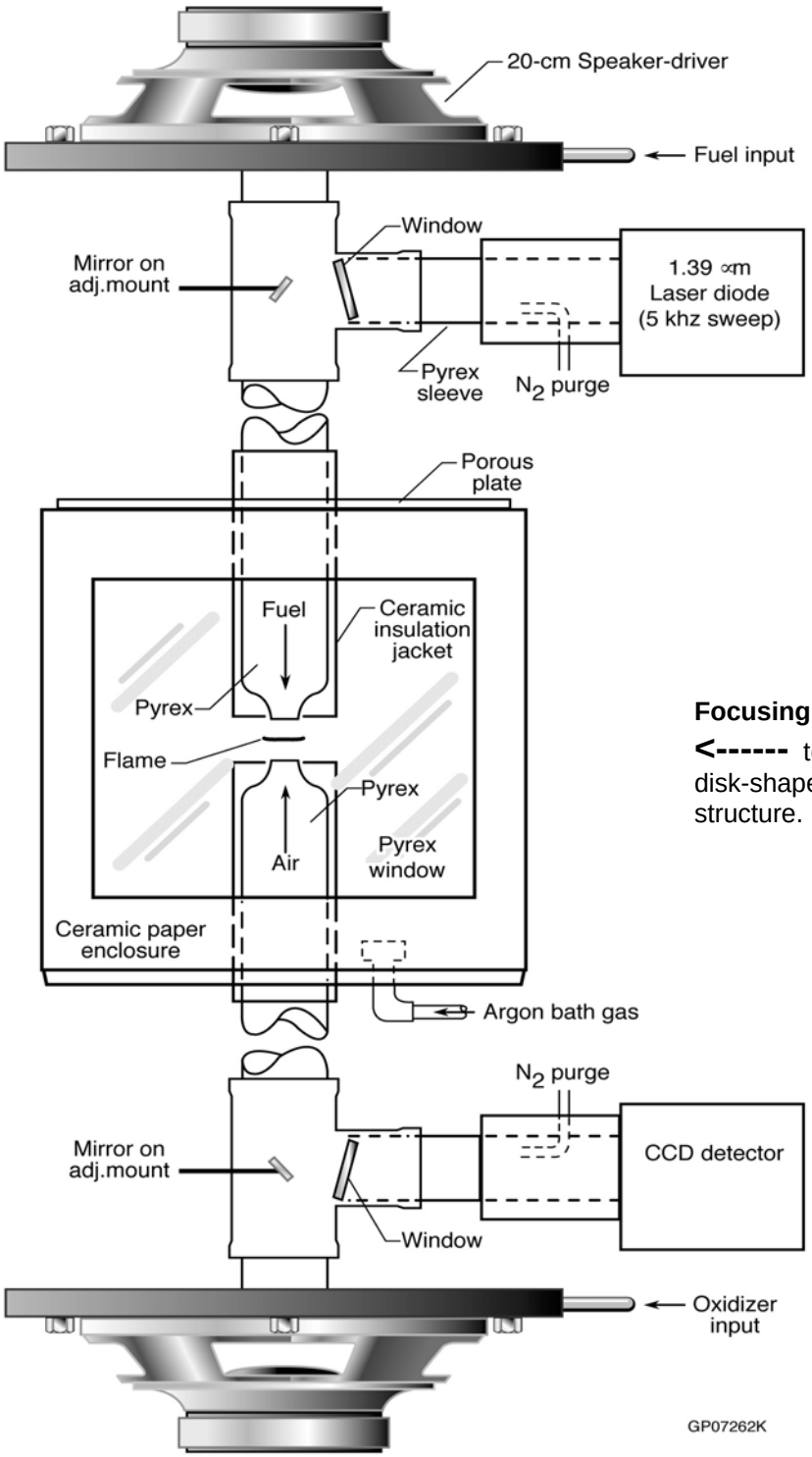

Focusing Schlieren System used continuously

<------ to visualize flows, including centering of disk-shaped flame, and vertical / horizontal structure. Details in [26,35,36]

Fig. 5a. Schematic of the Oscillatory Opposed Jet Burner (OOJB) system with twin 20-cm speaker-drivers, used to determine both steady-state FS and Dynamic Flame Weakening. Diode laser system is passive in this study.

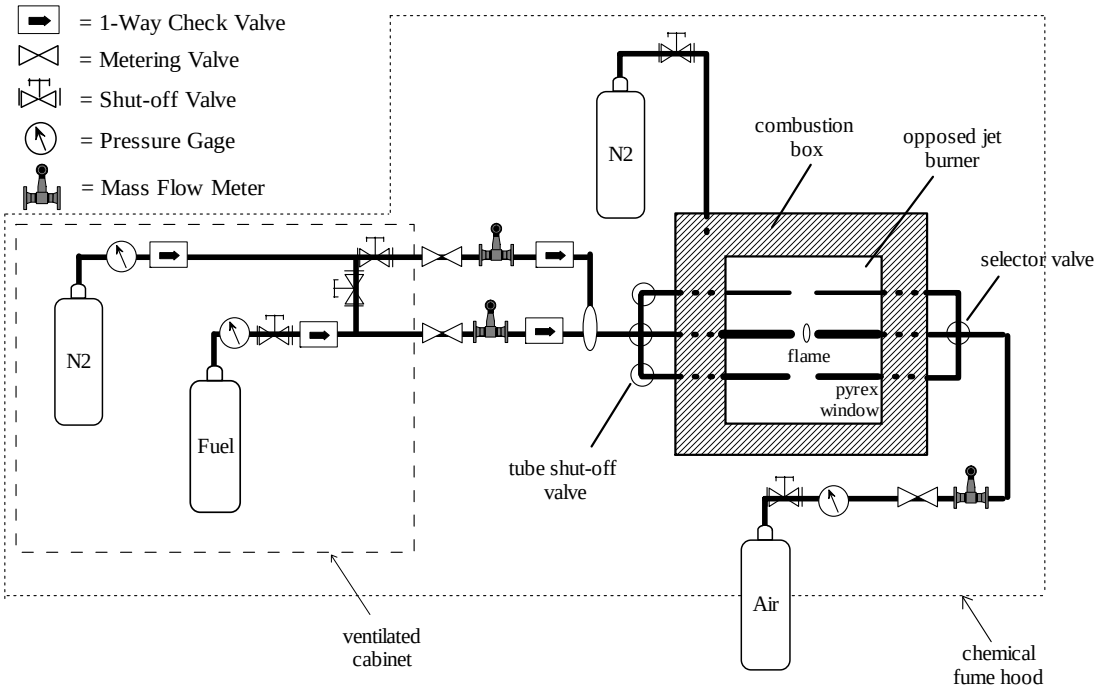

Fig. 5b. Gaseous-fuel horizontal-tube OJB test schematic (not to scale). Combustion box, constructed of 0.5 in thick compacted silica fiber-board panels, has a porous metal plate on top -- typically 4 x 6 in -- is exposed and "active". Thus combustion products are actively purged by controlled nitrogen flows from two porous plug outlets at opposite corners of the box floor. The three matching sets of tube-OJBs are actually arrayed in a horizontal plane, not vertically as shown. Mass flows of fuel, fuel-diluent, and air are monitored as flame extinction and restoration limits are approached and achieved.

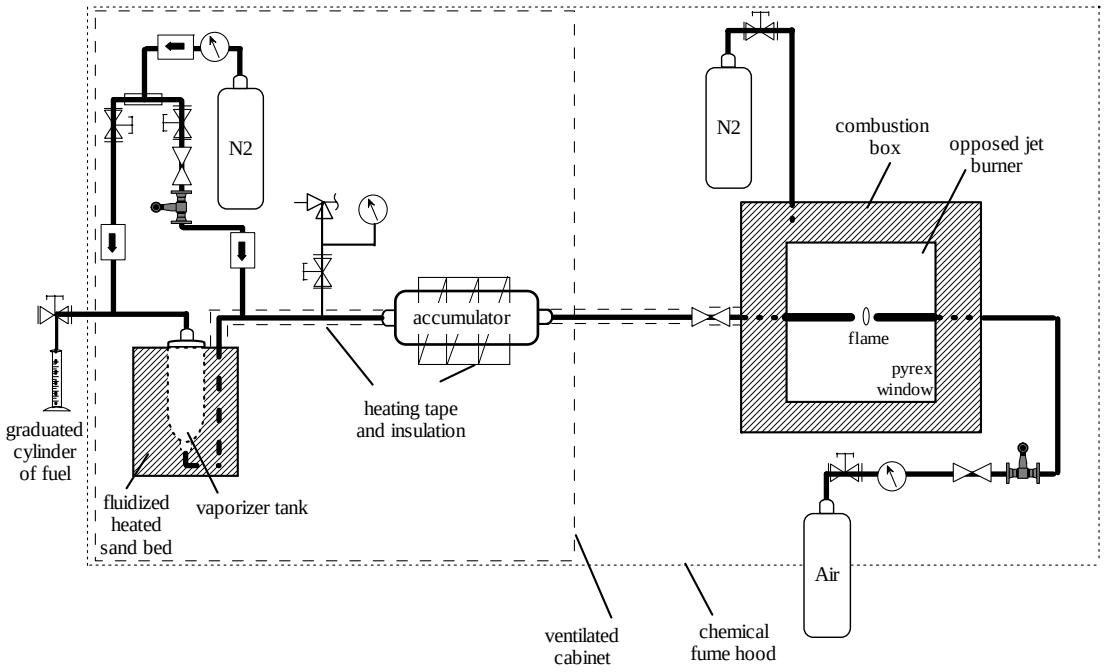

Fig. 5c. Liquid-fueled OJB test schematic (not to scale). Silica fiber combustion box, with porous plate on top, is identical to that in Fig. 5b. Vaporizer tank is ~ 0.5 L and accumulator tank is ~ 10.1 L. For each batch test (set), a known volume of liquid HC is injected into the cold, evacuated system. Then mass-flow-metered fuel diluent (either N_2 or gaseous HC) is admitted, up to a specific pressure. Finally, the system is sealed and heated to a measured (multipoint) temperature and pressure, and held there to assure mixing before it is operated in a "blow down mode," to supply the 7.5 mm tube-OJB system. For the hot vaporized-fuel experiments, air mass flows are monitored, but mass flows of fuel mixture are not monitored due to temperature limitations.

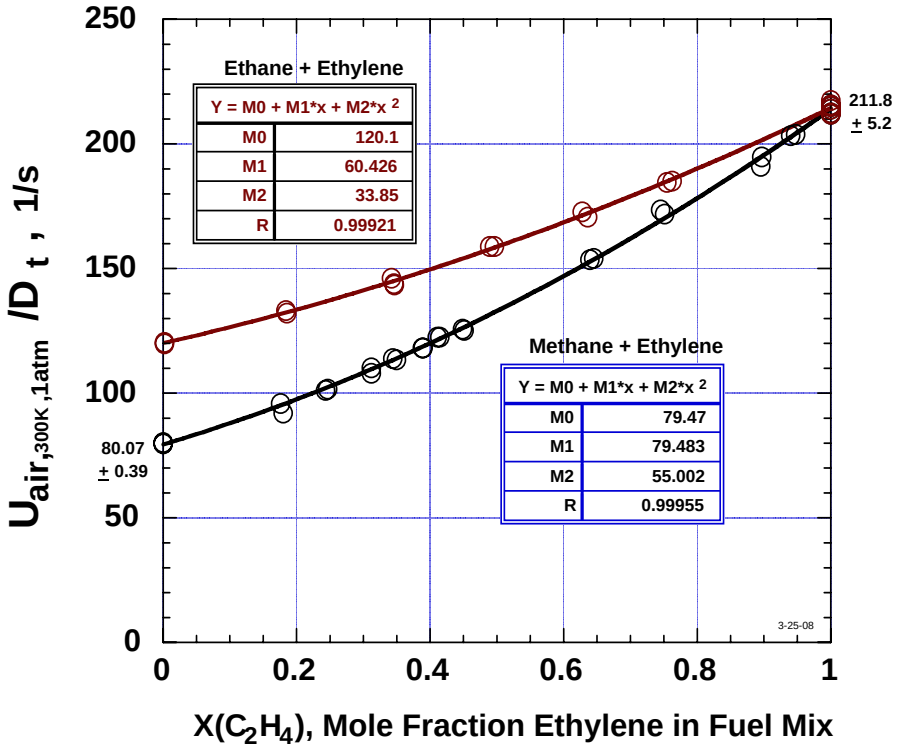

Fig. 6. Applied Stress Rates for Tube-OJB (ASR_t) at extinction for **Methane + Ethylene** *and* **Ethane + Ethylene** fuel mixtures vs Air CFDFs; 7.56 mm tube-OJB with 1 atm, 300 K inputs.

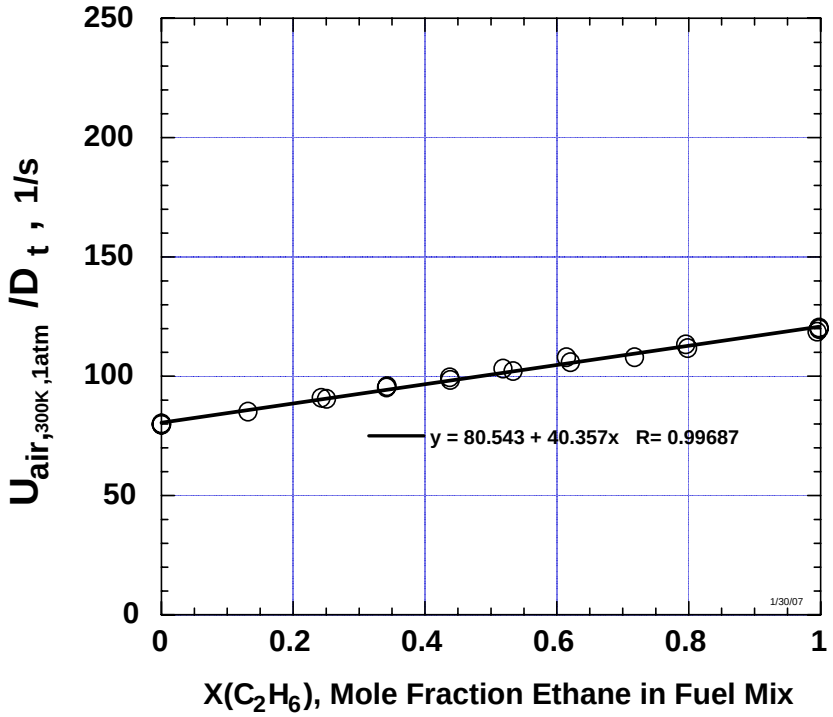

Fig. 7. ASR_t at extinction for **Methane + Ethane** fuel mix vs Air CFDFs; 7.56 mm tube-OJB with 1 atm, 300 K inputs.

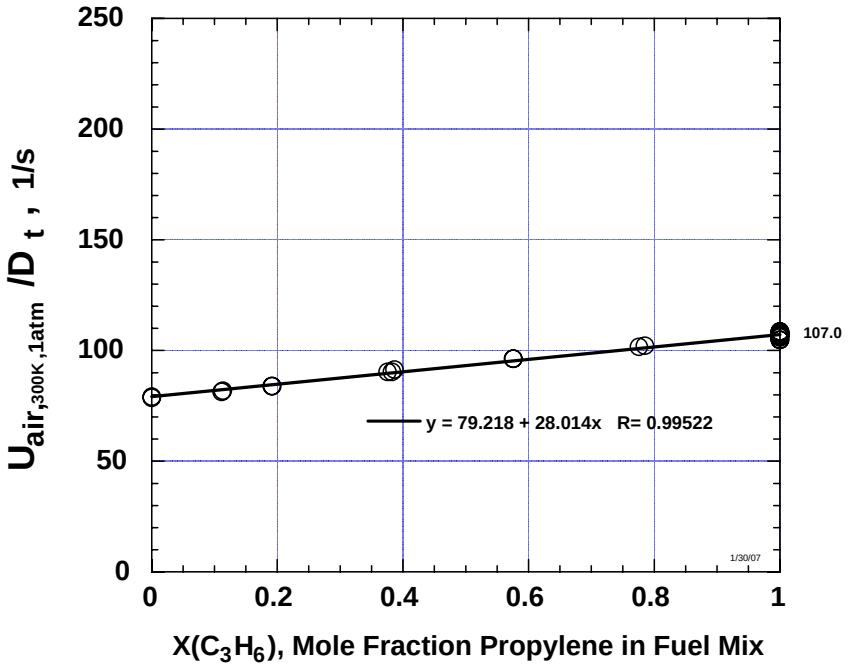

Fig. 8. ASR_t at extinction for **Methane + Propylene** fuel mix vs Air CFDFs; 7.56 mm tube-OJB with 1 atm, 300 K inputs.

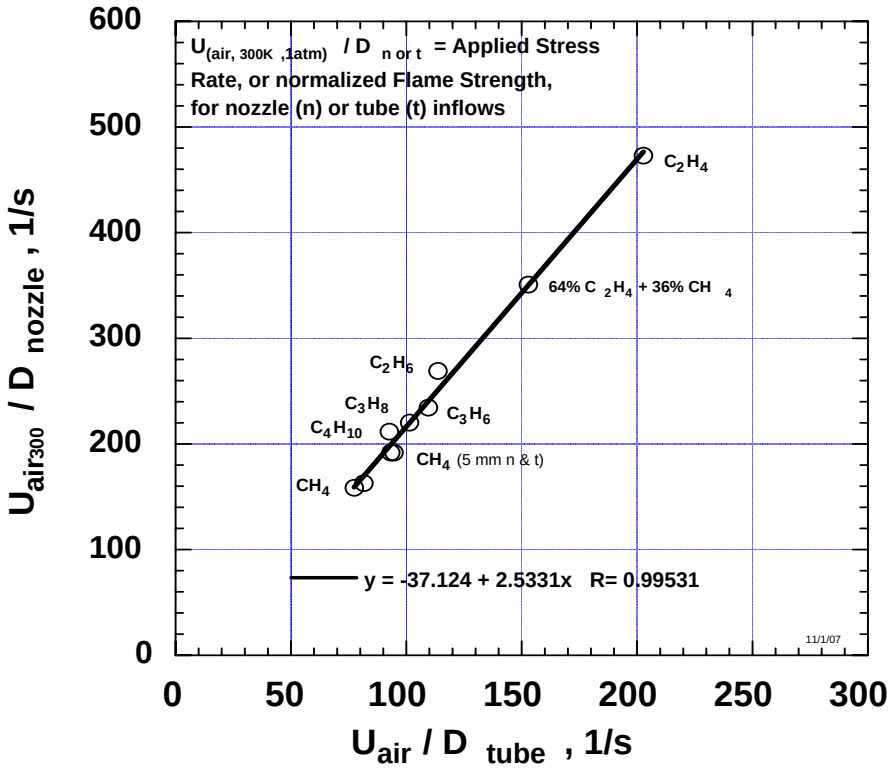

Fig. 9. OJB-extinction-limit "Idealized Flameholding Scale," with best linear fit, WITH intercept. ASRs from 7.2 mm convergent-nozzle- and 7.5 mm straight-tube-OJBs, for Methane, Butane, Propane, Propylene, Ethane, 64% Ethylene / 36% Methane mix, and Ethylene–Air CFDFs, with 1 atm, 300 K Air inputs.

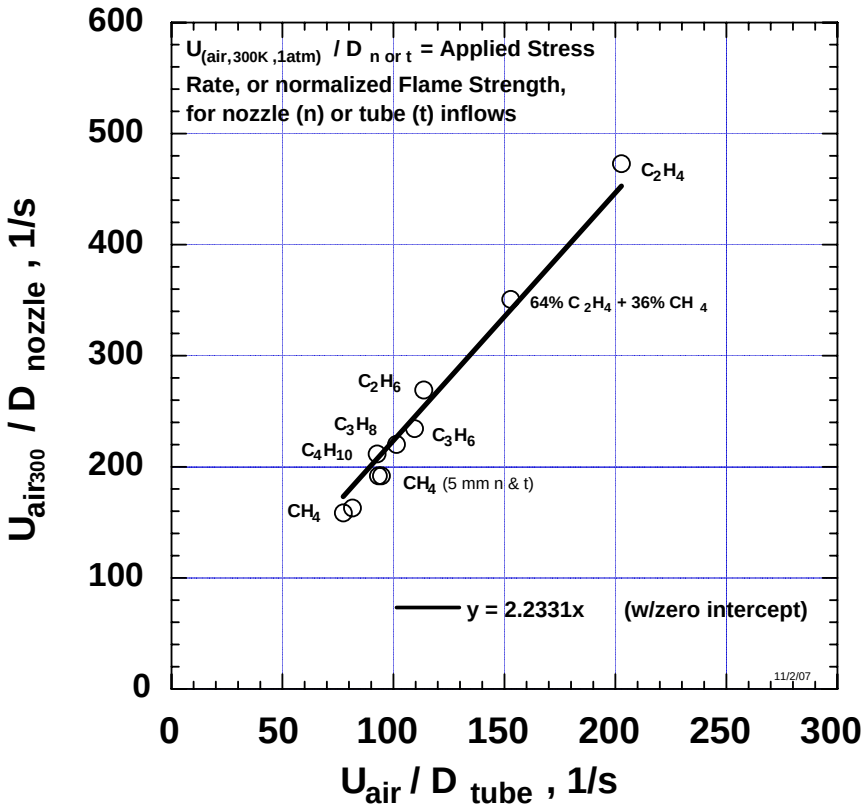

Fig. 10. OJB-extinction-limit "Idealized Flameholding Scale," with best linear fit, with zero intercept. ASRs from 7.2 mm convergent-nozzle- and 7.5 mm straight-tube-OJBs, for Methane, Butane, Propane, Propylene, Ethane, 64% Ethylene / 36% Methane mix, and Ethylene–Air CFDFs, with 1 atm, 300 K Air inputs.

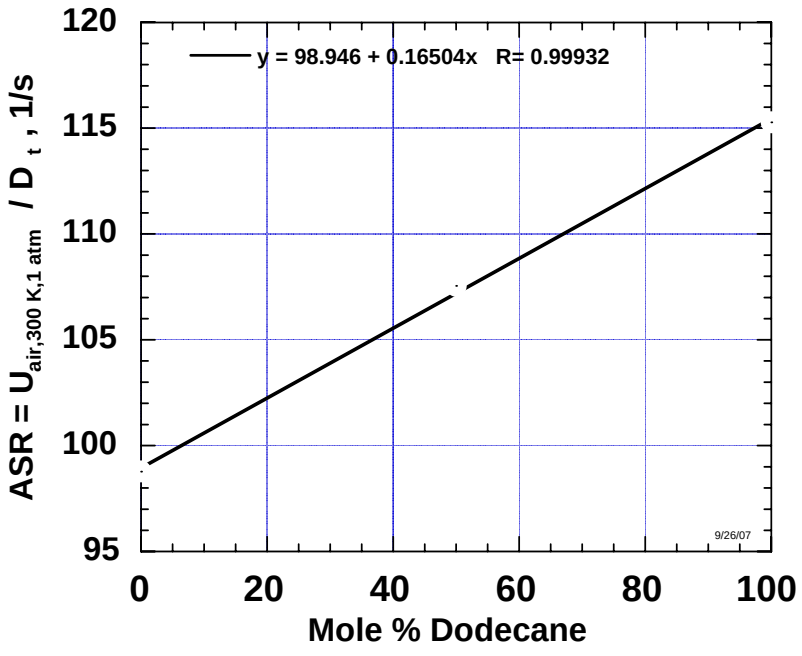

Fig. 11. ASR_t at extinction for 600 K ***n*-Heptane + *n*-Dodecane** vaporized fuel mixtures vs Air CFDFs; 7.56 mm tube-OJB with 1 atm, 300 K air inputs.

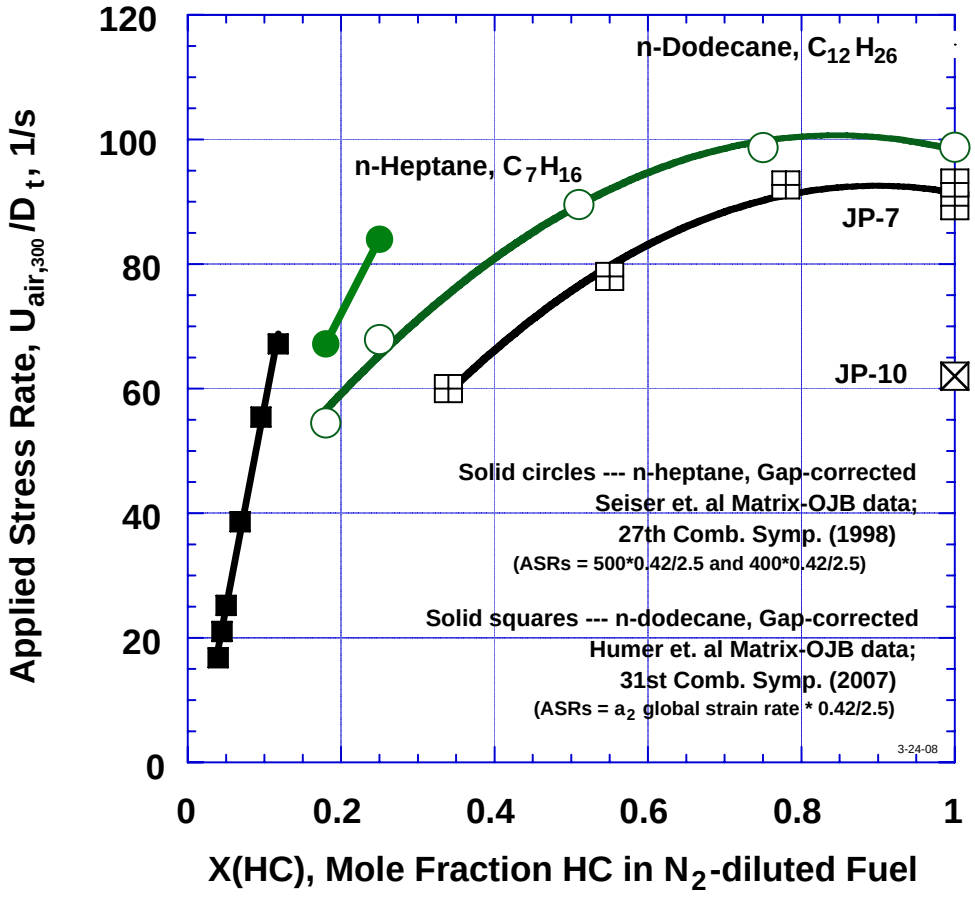

Fig. 12. ASR_t at extinction for 600 K N_2-diluted ***n*-Heptane, *n*-Dodecane**, and **JP-7**, and pure **JP-10** vaporized fuel mixtures vs Air CFDFs; 7.56 mm tube-OJB with 1 atm, 300 K air inputs. Note comparisons with gap-corrected UCSD Matrix Burner data, based on corrections discussed in Fig. A1.

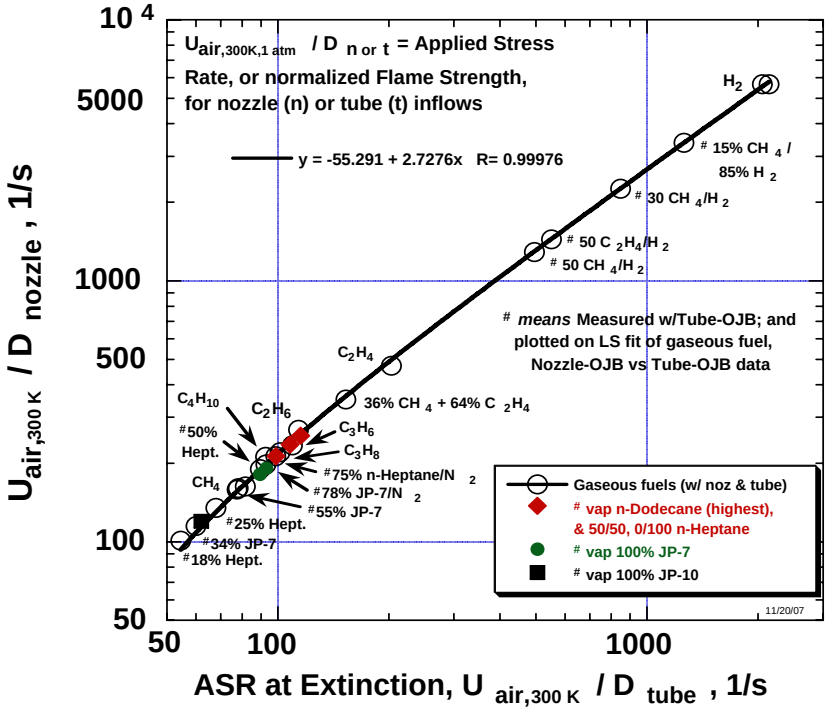

Fig. 13. ASR-based OJB-extinction-limit "Idealized Flameholding Scale" from convergent-nozzle- and straight-tube-OJBs, for JP-10, JP-7 / N_2, *n*-Heptane / N_2, *n*-Dodecane / *n*-Heptane mixtures; and Methane, Butane, Propane, Propylene, Ethane, 64% Ethylene / 36% Methane mixture, Ethylene, and Hydrogen–Air CFDFs, with 1 atm, 300 K air inputs.

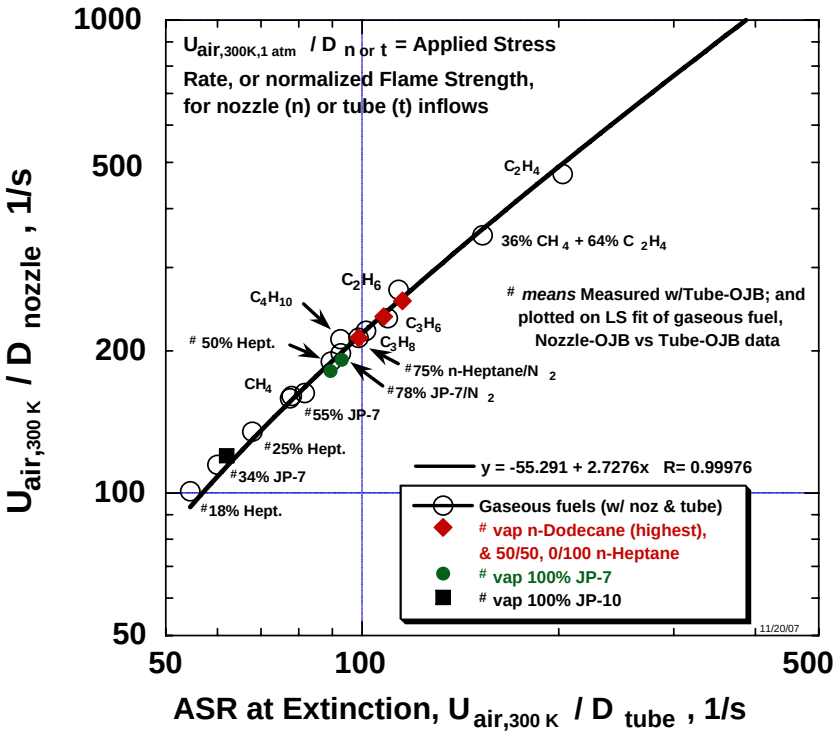

Fig. 14. Hydrocarbon portion of Fig. 13 ASR-based OJB-extinction-limit "Idealized Flameholding Scale" from convergent-nozzle- and straight-tube-OJBs, for various Fuel–Air CFDFs, with 1 atm, 300 K air inputs.

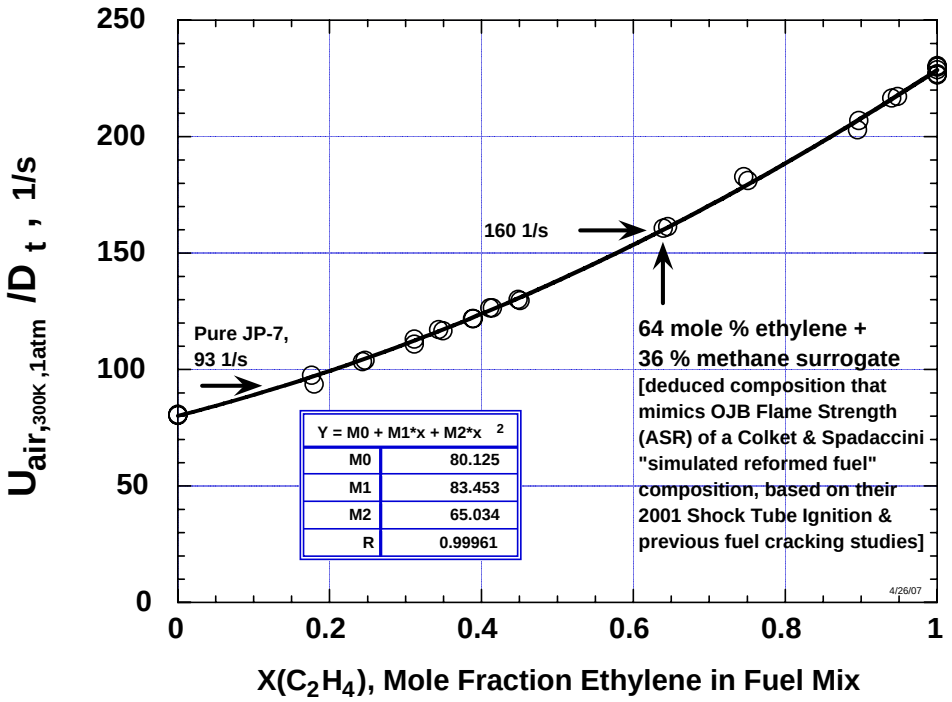

Fig. 15. ASR_t at extinction for **600 K Methane + Ethylene** fuel mix vs Air CFDFs; 7.56 mm tube-OJB with 1 atm, 300 K air inputs. Note pure JP-7 is equivalent to 15 mole % ethylene + 85% methane.

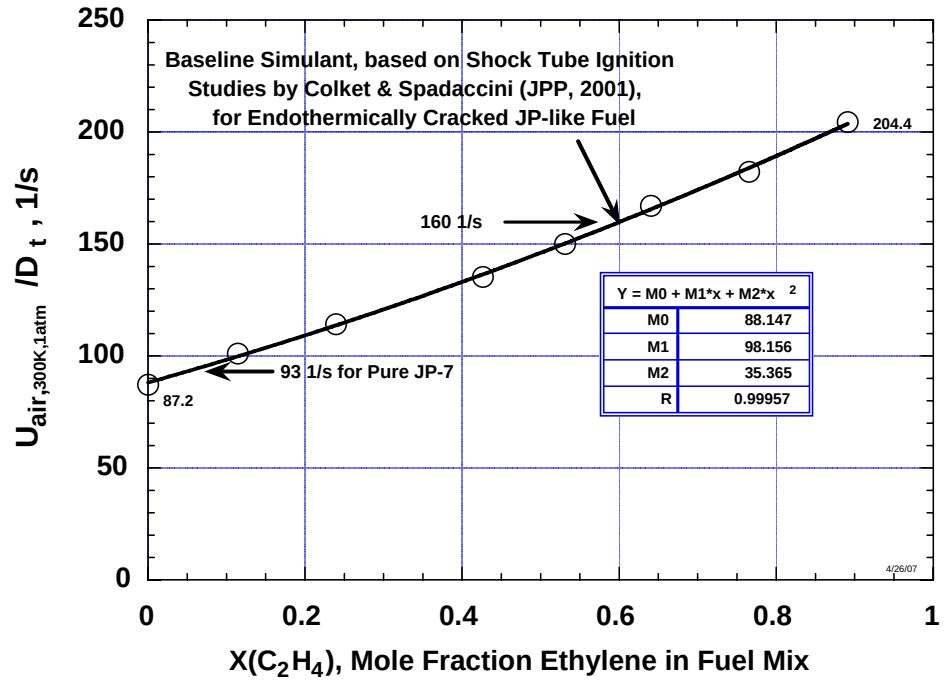

Fig. 16. ASR_t at extinction for **600 K Methane + Ethylene + 10.8 mole %** *n*-Heptane gaseous fuel mix vs Air CFDFs; 7.56 mm tube-OJB with 1 atm, 300 K air inputs.

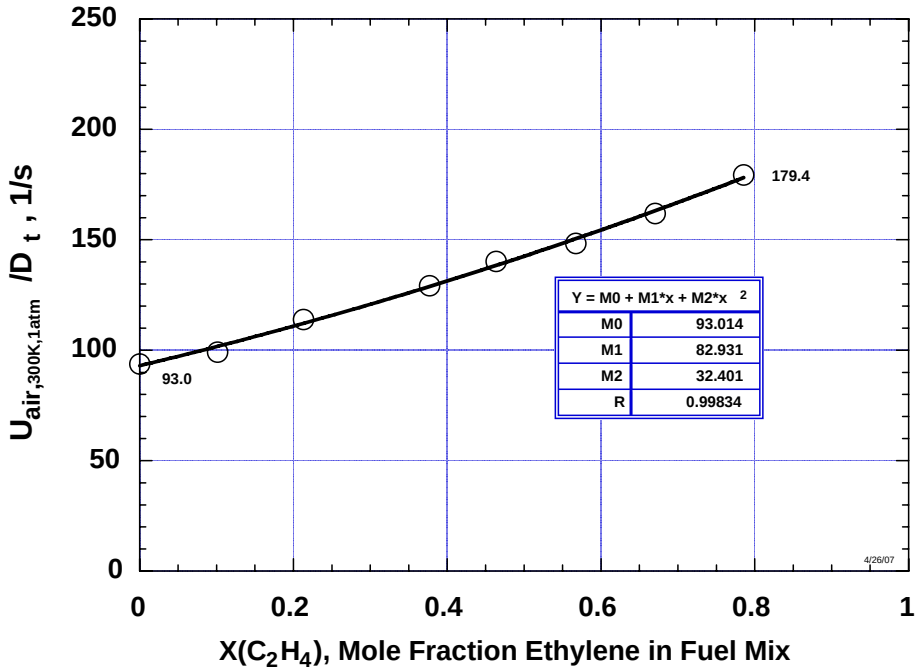

Fig. 17. ASR_t at extinction for **600 K Methane + Ethylene + 21.3 mole % *n*-Heptane** gaseous fuel mix vs Air CFDFs; 7.56 mm Tube-OJB with 1 atm, 300 K air inputs.

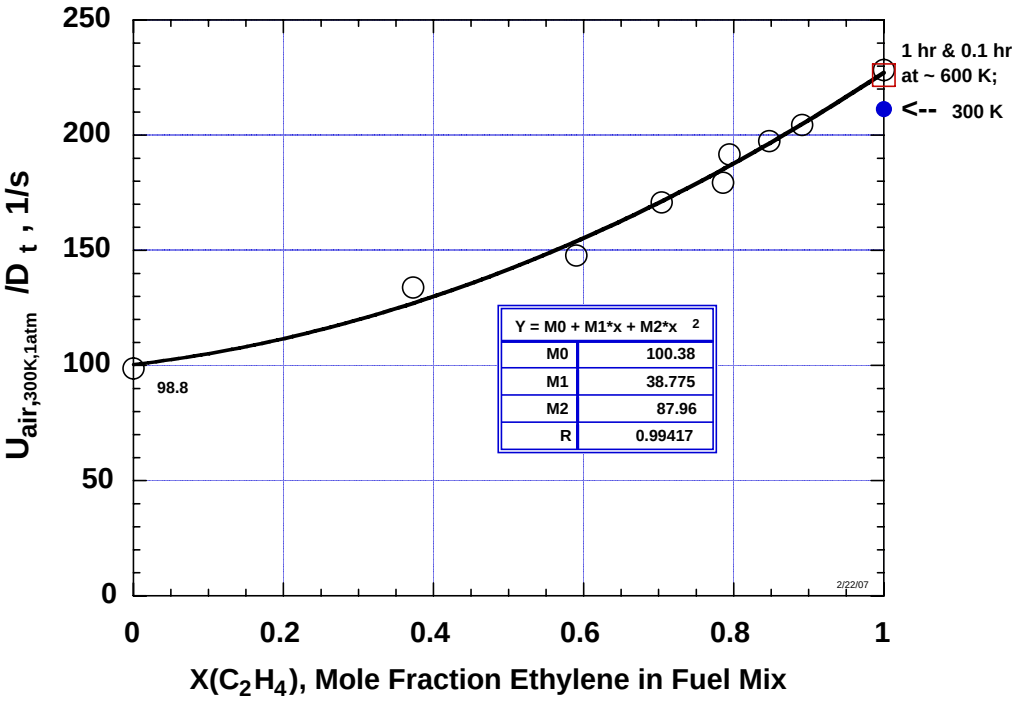

Fig. 18. ASR_t at extinction for **600 K *n*-Heptane + Ethylene** gaseous fuel mix vs Air CFDFs; 7.56 mm tube-OJB with 1 atm, 300 K air inputs.

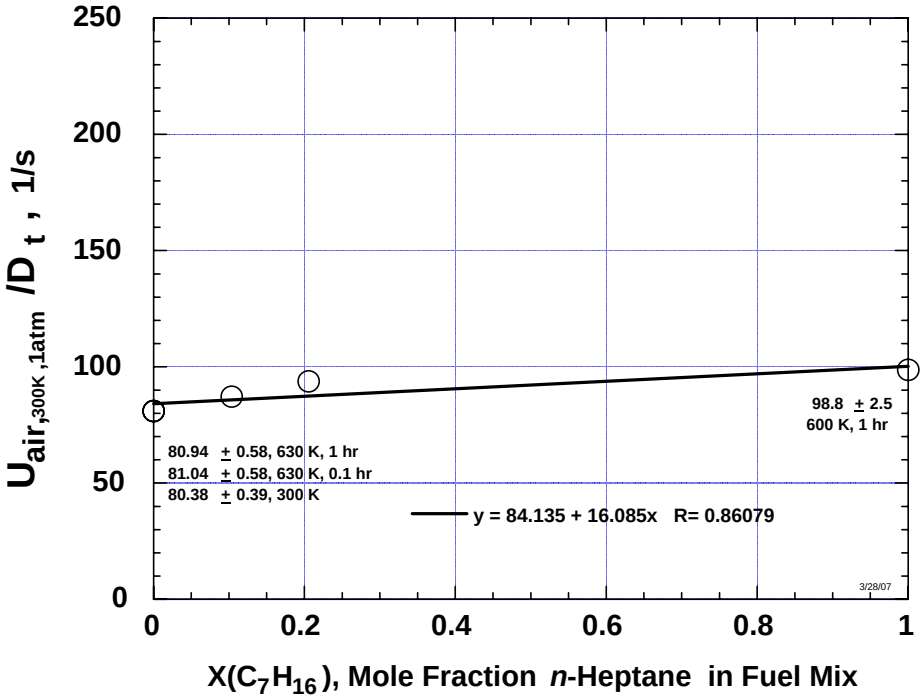

Fig. 19. ASR_t at extinction for **600 K *n*-Heptane + Methane** fuel mix vs Air CFDFs; 7.56 mm tube-OJB with 1 atm, 300 K Air Inputs. Note the very small effect of heating methane for 0.1 hr or 1 hr "reaction" times.

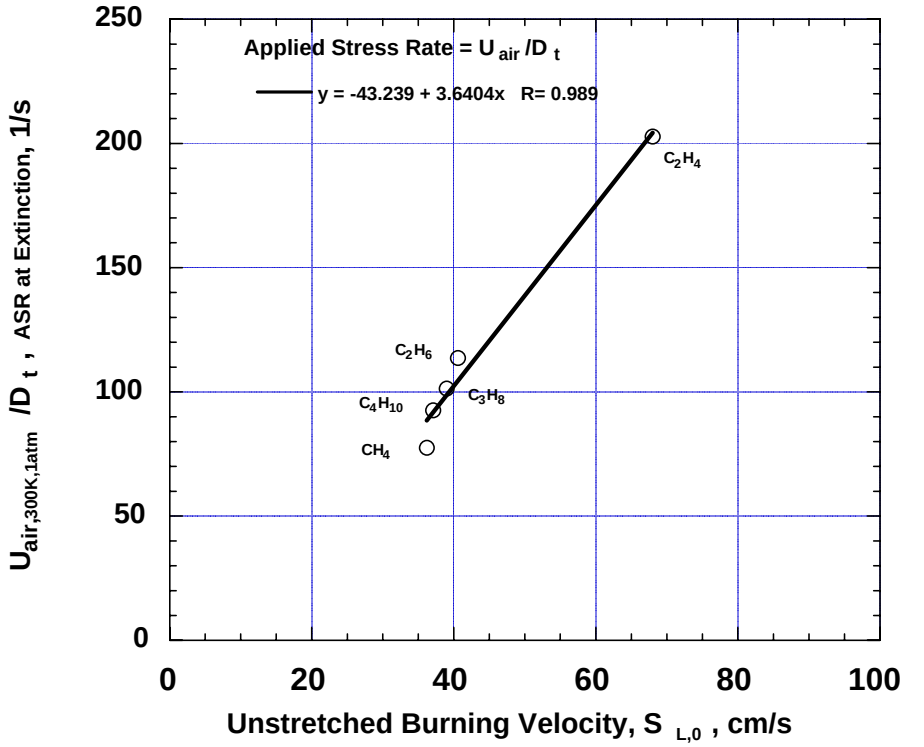

Fig. 20. Comparison of extinction limits, from 7.5 mm tube-OJB, with unstretched Laminar Burning Velocity at phi = 1, for Methane, Ethane, Propane, Butane and Ethylene–Air flames.

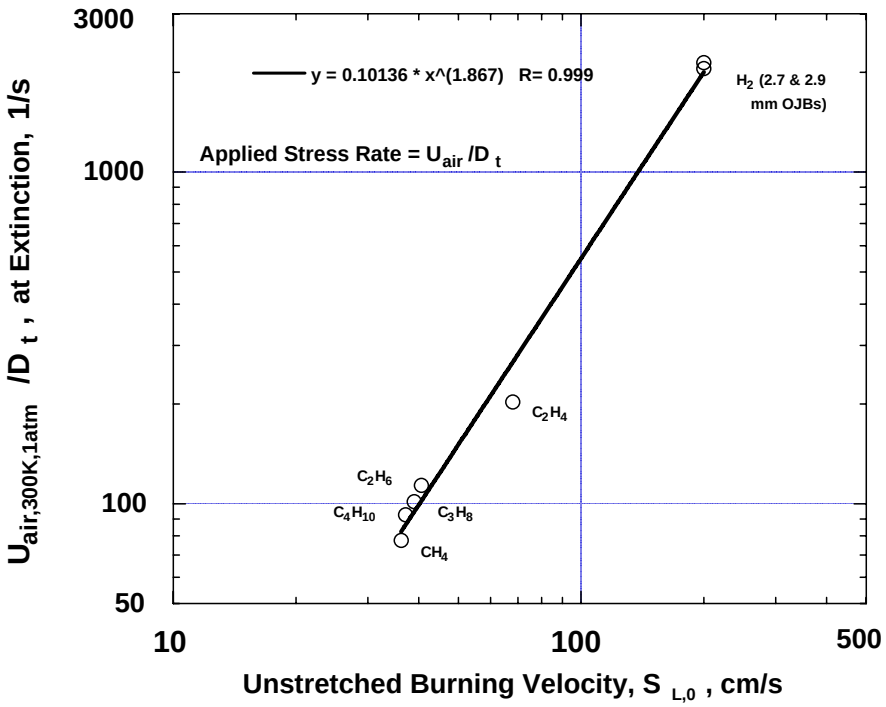

Fig. 21. Comparison of extinction Limits, from 7.5 mm tube-OJB, with Un-Stretched Laminar Burning Velocity at phi = 1, for Methane, Ethane, Propane, Butane, Ethylene **and** H_2–Air flames.

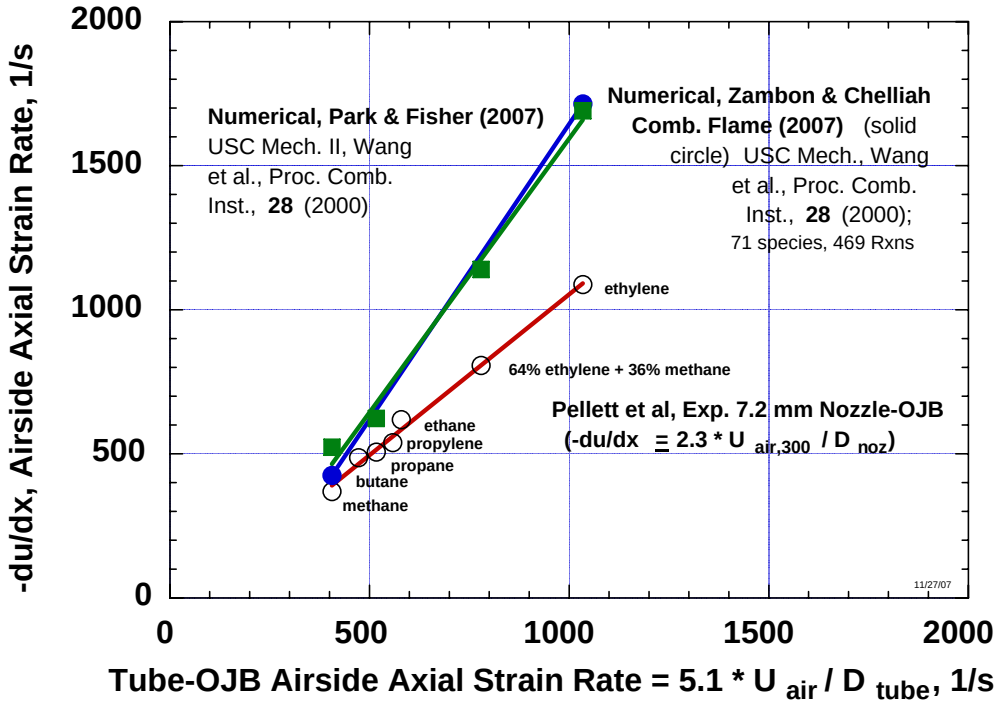

Fig. 22. Comparison of experimental and numerically simulated strain induced extinction limits for Fuel vs Air CFDFs at 1 atm, using the best estimate global measures of airside axial strain rate (see development of Eq. (2) in text.)

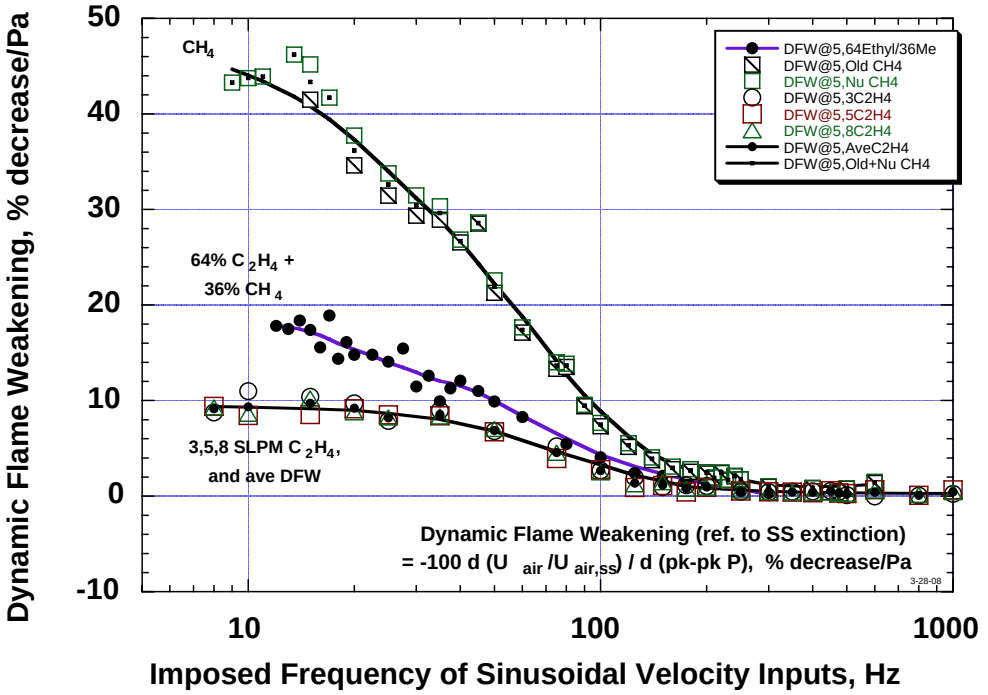

Fig. 23. Dynamic Flame Weakening, for extinction of C_2H_4, CH_4, and 64% C_2H_4 / 36 % CH_4 Surrogate vs Air CFDFs, using 7.2 mm Pyrex Nozzle OOJB and Axially-Applied Sinusoidal Velocity (Pressure) Inputs probed by Microphone (cal @ 5 SLPM)

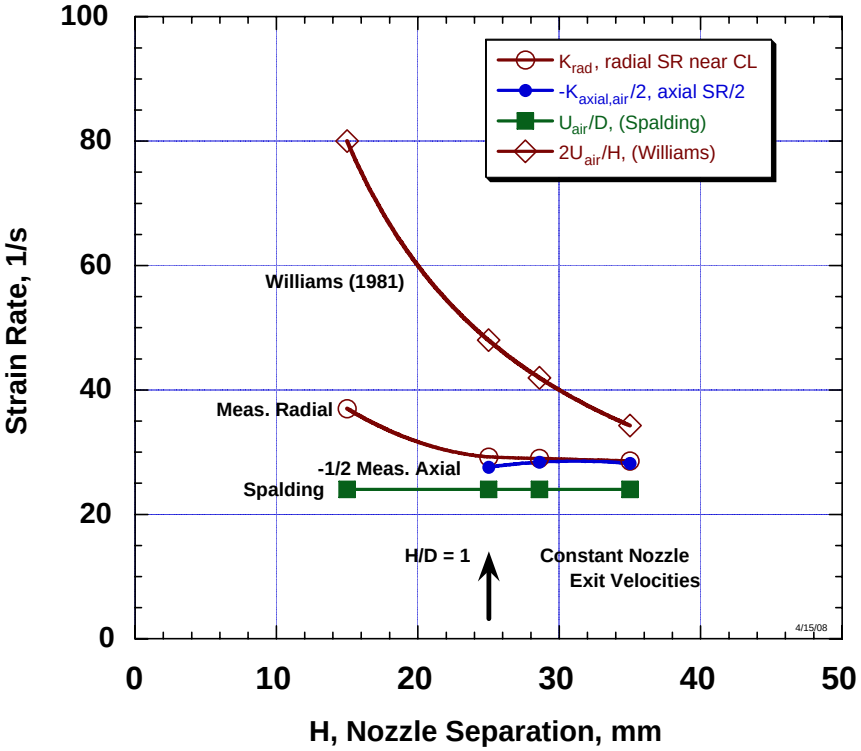

Fig. A1. Comparison of Rolon's LDA-measured Strain Rates for variable separation of 25 mm contoured nozzles, Air vs Air [52]. For $H/D_n \geq 1$, the radial and -1/2 axial strain rates approximately equal 1.15 U_{air}/D_n, which agrees with recent numerical simulations [41].

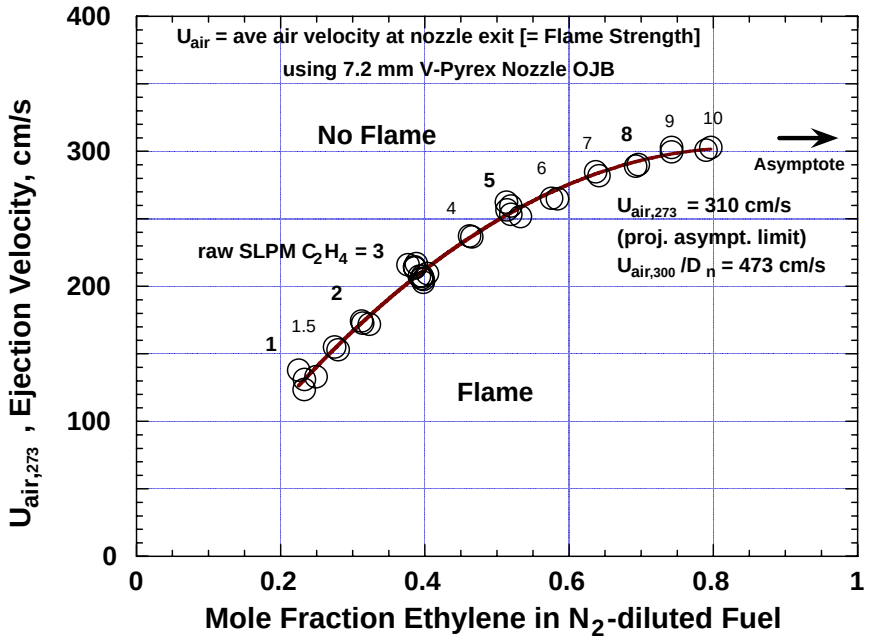

Fig. A2. Steady-state extinction of C_2H_4/N_2–Air CFDFs, using 7.2 mm vertical-Pyrex nozzle Oscillatory-OJB system.

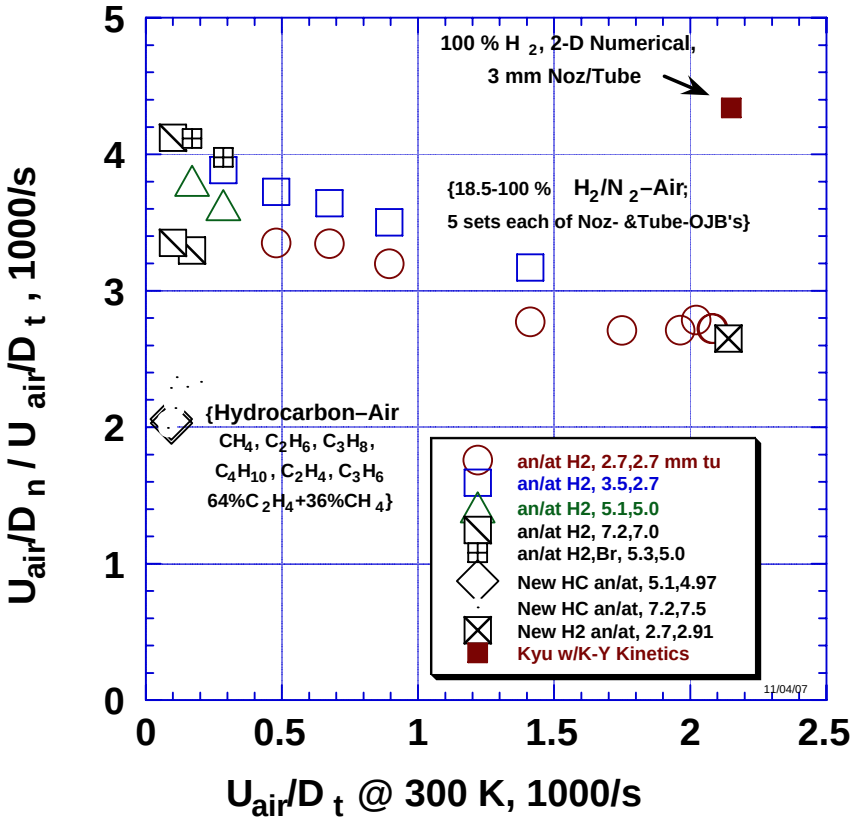

Fig. A3. Summary plot of ratio of Applied Stress Rates at extinction for nozzle-OJBs / tube-OJBs, as a function of ASR_t for tube-OJBs, for hydrogen–air *and* hydrocarbon–air data.